©2013

Grace D. Bundens

ALL RIGHTS RESERVED

FROM BODY TO ROOT: ALTERNATIVE FABRICATION TECHNIQUES AND ATTACHMENT MECHANICS FOR A TISSUE ENGINEERED MENISCUS CONSTRUCT

by

GRACE DOROTHY BUNDENS

A thesis submitted to the

Graduate School-New Brunswick

Rutgers, The State University of New Jersey

and

The Graduate School of Biomedical Sciences

University of Medicine and Dentistry of New Jersey

in partial fulfillment of the requirements

for the degree of

Master of Science

Graduate Program in Biomedical Engineering

written under the direction of

Michael G. Dunn, Ph.D.

and approved by

_____

_____

_____

New Brunswick, New Jersey

OCTOBER, 2013

ABSTRACT OF THE THESIS

From Body to Root: Alternative Fabrication Techniques and Attachment Mechanics for a Tissue Engineered Meniscus Construct

By GRACE D. BUNDENS

Thesis Director:

Michael G. Dunn, Ph.D.

Meniscal tears increase joint cartilage strains and contribute to the development of osteoarthritis of the knee. Tears within the meniscal body and at the root result in altered load transmission and cartilage damage, elucidating the need for tissue-engineered solutions. The first part of this study aims to examine the effect of meniscal scaffold fabrication techniques on the mechanical properties of poly (DT DDD) fibers. Electrospinning will also be evaluated as a new fabrication technique for partial meniscus replacements, preserving more native tissue than previous tissue-engineered solutions. Finally, the ovine meniscal root will be characterized in order to strengthen large animal model trials. While the human meniscus has been well characterized, little is known about the ovine meniscus, a model commonly used in orthopaedic research. Implants are more likely to fail during pre-clinical testing when their fixation technique does not take the modelôs native biomechanics into account. Increased knowledge of scaffold fabrication techniques and the ovine meniscus will allow for better adaptation of tissue-engineered replacements to a large animal model, a crucial step prior to human clinical trials.

Dedication

For my family,

If you are only to read one page of this work, make it this:

To my parents,

David and Connie Bundens,

who selflessly put my needs and education above all else

and raised me to know the importance of hard work and determination,

Your unwavering love and support has made all things possible.

and to my Grandmother,

Virginia Harper,

who has always believed in me

and taught me the true meaning of gumption.

Acknowledgements

I would first like to acknowledge my advisor Dr. Michael G. Dunn who provided me with great support and guidance over the past two years. He allowed me the freedom to combine my biology background with medical interests, while always keeping an eye on the bigger clinical picture. His positive energy, jeopardy knowledge, and softball game were truly inspirational. I would also like to especially thank Dr. Charles Gatt who would often slip away from his other duties to provide clinical insight on our research and I am very appreciative of the time I spent learning from him in the OR. His tireless efforts to balance a clinical practice, surgical department, research, and family is something I can only hope to emulate in the future. I would also like to thank Dr. Freeman for sharing his expertise on electrospinning with our lab. His generosity has been much appreciated. I recognize the sacrifice of my committee membersô time for the benefit of my thesis.

This work would not have been possible without the many undergraduate, graduate and medical students of the Dunn lab. Special thanks to the lab originals, Aaron ñSpiritò Merriam and Aaron Seto, who spent countless hours teaching me everything I know from harvests to mechanical testing to softball. As someone who arrived with no engineering background and strong personality, it could not have been easy but I am forever grateful for your mentorship. To the soon-to-be senior members of the Dunn lab, Jay Patel and Justin Rice, you have been wonderful colleagues and inevitably make every day at work more enjoyable. The friendship of these four has been a most valuable part of my graduate experience, thanks for letting me into the boys club. I will miss our close-knit group, from competitive card games, hiking trips, and lunch walks to happy hours

and sports leaguesð Go Osteoblasts! I am also grateful to the other students who assisted through the years and made the day-to-day experience more fun. Special thanks to Steven Brousell, for his contributions to this project and advice, along with the new kids on the block: Chris Mino, Dave Macknet, Bridget Natalicchio, and Ami Sawhney.

I am also extremely grateful to members of our extended Ortho family. Barbara Perry and Don Thompson have always indulged my medical interests and spent many hours teaching me the surgical skills that I will carry into my medical career. Thanks to Michelle Allen, who managed everyday tasks and was a welcoming presence from the day I started. Additionally, I would also like to acknowledge Dr. Freeman and members of his MoTR lab, Brittany Taylor and Kristin McKeon, for their training and assistance in the art of electrospinning.

I have also had the great fortune of meeting an exceptional group of colleagues that I am pleased to call friends: Laura Higgins, Kathryn Drzewiecki, Kate Fitzgerald, and Maria Qadri. It seemed improbable that I would share my classes with not one but four women who would become wonderful friends. Each of these individuals contributed to my success as they patiently helped, encouraged, and, when necessary, forcefully dragged me out and without them, Iôm certain I would not have made it. Above all else, I am truly grateful for their friendship and support over the last couple of years, which has gone a long way to preserve my sanity.

Finally, all of this would not have been possible without the support of my family. I would like to thank my parents, David and Connie Bundens, who have always supported my academic pursuits. Your encouragement and belief in my abilities helped

me through this process. I would not be approaching the conclusion of my graduate career and the start of my next academic adventure if it werenôt for you.

Table of Contents

LIST OF TABLES

LIST OF ILLUSTRATIONS

CHAPTER 1: INTRODUCTION

1.1 Meniscus Gross Anatomy and Function

The menisci of the knee are two crescent-shaped fibrocartilaginous tissues that function in stability, lubrication, and joint health (Figure 1-1). They provide structure to the knee joint and distribute femoral loads across the tibia[1,2]. The menisci undergo complex loads such as tension, compression, and shear[3,4]. The composition of this tissue as well as its firm attachments enables the transmission of such forces[5] (Figure 1-2).

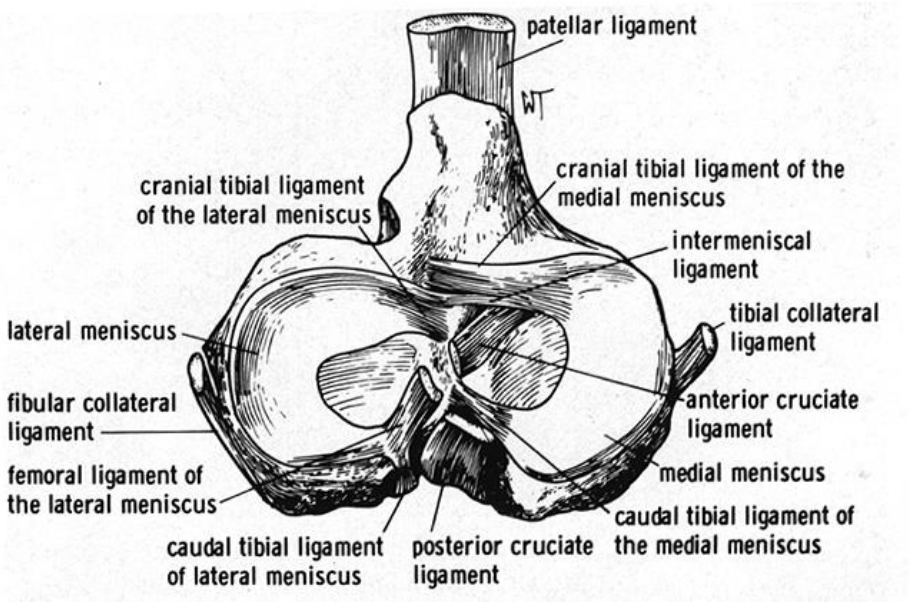

Figure 1-1: Drawing of dorsal aspect of tibia in an animal, superior aspect in humans, illustrating the meniscal attachments. Figure adapted from Arnoczky[6].

The meniscus has a triangular cross-section and consists of matrix molecules such as glycosaminoglycans (GAGs) and collagen and gains cushioning and lubricating effects due to the properties of these molecules[7]. While the peripheral third is vascularized by way of the medial or lateral genicular artery, the inner two thirds is relatively avascular and nourished by synovial fluid[8]. Studies have shown there is variation across the regions

of the meniscus in GAG coverage, collagen type, and cellular density. However, the meniscus is composed predominantly of type I collagen.

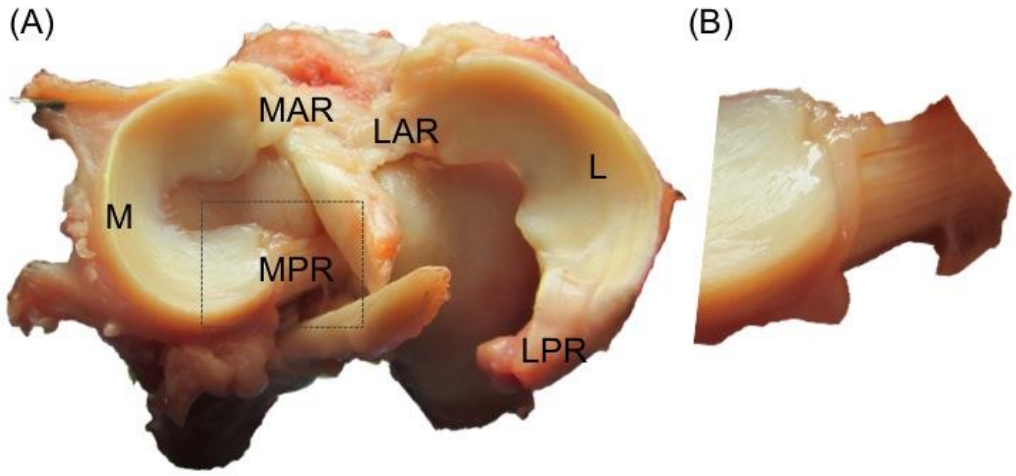

Figure 1-2: Relevant meniscal anatomy from a sheep tibia. Lateral posterior root's femoral insertion has been bisected. (M-medial meniscus, L- lateral meniscus, MAR- medial anterior root, MPR- medial posterior root, LAR- lateral anterior root, LPR- lateral posterior root) (B) Close up of posterior attachment of medial meniscus.

The menisciôs collagen fibers are predominantly arranged circumferentially, however there are also radially aligned fibers and a superficial unorganized meshwork of collagen (Figure 1-3). The circumferential fibers function to dissipate femoral loads through the production of hoop stresses in the menisci. Both the circumferential and radial fibers allow the meniscus to expand in compression, increasing the contact area of the joint[8]. The circumferential fibers oppose the tensile deformation while the GAGs oppose the compressive deformation[9,10]. The combination of these opposing forces

results in increased contact area with a decrease in the peak forces along the tibial plateau.

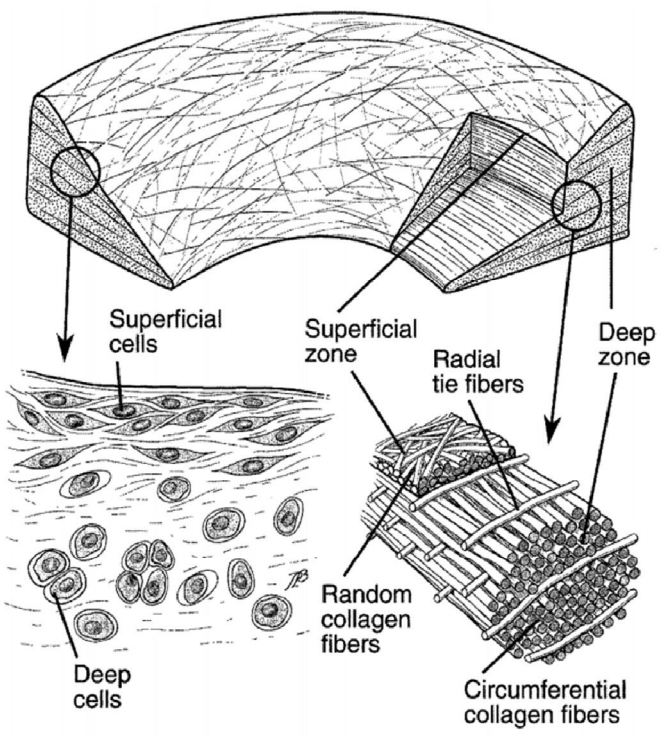

Figure 1-3: Collagen fiber arrangement within the meniscus. Figure adapted from Kawamura[11].

1.2 Pathophysiology of Meniscal Tears

Meniscal tears are the most common injury to the knee requiring surgery[8,12], occurring three times more often in the medial meniscus than in the lateral meniscus. Both meniscal tears and meniscectomy have been shown to increase the rate of osteoarthritis[13-16]. Meniscal tears are classified according to their position relative to the periphery, as the vascular supply is the primary determinant of its healing capacity, as well as their morphology. The vascular periphery experiences a higher potential for healing and can be repaired. In addition to tears of the meniscal body, root tears

completely disrupt the circumferentially aligned fibers resulting in meniscal extrusion. Posterior root tears have been shown to be biomechanically equivalent to complete meniscectomies[17]. This disruption of meniscal congruity results in decreased contact area and increased peak loads on the tibial plateau, leading to an increased risk of cartilage damage and osteoarthritis[18-21]. As these tears are seen in a variety of age ranges and activity levels, treatments need to provide long-term chondroprotection and symptom relief.

1.3 Treatment of Meniscal Tears

Despite their prevalence, meniscal tears are not easy to repair using sutures. As a result the meniscus is usually partially or completely removed (meniscectomy). However, meniscectomy has been shown to decrease the contact area and increase the forces on the tibial plateaus, stressing the underlying cartilage and resulting in an increased risk for osteoarthritis[22]. Therefore surgical approaches aim to restore normal contact forces while alleviating the pain associated with meniscal instability.

Degenerative, complex and central radial tears are typically treated with partial meniscectomy. During this procedure a minimal amount of meniscus is resected to create a smooth transition zone. Surgeons aim to preserve as much normal meniscus as possible in order to decrease the biomechanical impact on the joint. Peripheral longitudinal tears are usually repaired and while there are several techniques for this procedure, the inside out technique with vertical mattress sutures remains the ñgold standardò. Repairs have been shown to be anywhere from 30-90% successful depending on location, tear classification, ACL status, and chronicity[8,23-25]. The best results have been reported in

young patients with a peripheral tear and concurrent ACL reconstruction. Meniscal transplantation is a controversial procedure indicated for young patients presenting with symptoms of chondrosis and near complete meniscectomy[8,26]. The implant is fixed with either bone plugs or a bone bridge encompassing both attachments[27,28]. However, implants must be properly sized for each patient and the procedure is indicated for a very limited patient population. The abundance of meniscal injuries and the lack of a satisfactory treatment create a clinical need for a tissue engineered meniscus replacement.

1.4 Scaffold Based Meniscal Tissue Engineering

Currently, there is no FDA approved meniscus replacement available for use in the United States. However there are two products approved for use in Europe: Actifit and Menaflex/Collagen Meniscal Implant (CMI)[29-39]. Actifit is a polyurethane based sponge and indicated for limited use in partial meniscus replacement. CMI is a collagen-based sponge also approved for use in partial meniscus replacement. While they have seen promising results, as a porous, mold-formed scaffold they neglect certain aspects of the mechanical loading conditions experienced by the meniscus, which has led to mixed reviews. Both scaffolds are incapable of reproducing the hoop stresses that develop in normal menisci and instead act as a cushion. Additionally, degradation of polyurethane has been shown to impede the formation of neo-cartilaginous tissue[29-31,33-35]. While CMI has shown promise with neo-tissue formation, the collagen scaffold rapidly degenerates and leaving tissue that is not ready to act as a normal meniscus. Additionally long-term results conducted by independent sources have not been reported.

To recapitulate the native hoop stresses, the Orthopaedic Research Lab at Robert Wood Johnson hospital began incorporating polymer fibers into their design, providing better degradation profiles and mechanical properties (Figure 1-4).

Figure 1-4: Polymer-reinforced collagen sponge scaffold from Orthopaedic Research Lab at Robert Wood Johnson Hospital. Left side reveals the quasi-woven structure while the right side shows the scaffold after injection of the collagen sponge and rehydration prior to implantation surgery. Image courtesy of Aaron Merriam (Orthopaedic Research Lab, New Brunswick, NJ).

CHAPTER 2: The effect of production techniques on polymer fibers for tissue engineered meniscus scaffolds

2.1 Rationale

This thesis aims to evaluate scaffold materials in order to enhance the current hybrid synthetic polymer fiber and enhanced collagen sponge scaffold used in the lab at RWJ. Once woven into a meniscus-like structure, the polymer fiber is exposed to several different ñtreatmentsò along the way to surgical implantation (Figure 2-1). While the mechanical properties of the p(DTD DD) fiber used are well known, little is known about the effects of the treatments on the polymerôs material properties.

2.2 Objective

This study aims to evaluate the mechanical changes of individual polymer fibers due to meniscus scaffold production techniques. Each processing step will mirror the protocols used at RWJ and employ individual as well as combinations of treatments in order to elucidate their effects and attribute causal relationships to observed results. The changes will be determined using mechanical testing. Ultimately, the overarching goal of this thesis is to determine the best polymer scaffold production technique for success in a large animal model.

2.3 Hypotheses

Null Hypothesis: Meniscus scaffold preparation techniques will not affect the mechanical properties of individual polymer fibers.

2.4 Materials and methods

This study aimed to evaluate the effects of scaffold production techniques on individual p(DTD DD) fibers. Validation was based on preservation of mechanical properties, as this is a necessary feature of successful implants. Five individual processing conditions and three combinations were tested on individual polymer fibers and their mechanical properties were compared with untreated fibers. All experiments were carried out at room temperature.

Each processing condition described below was carried out in accordance with the protocols developed in the Robert Wood Johnson Orthopaedic Laboratory for use in meniscus scaffold fabrication. This process is diagramed in (Figure 2-1).

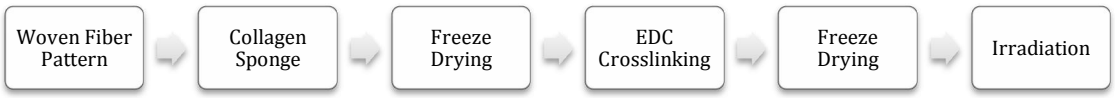

Figure 2-1: Meniscus scaffold processing techniques.

As the polymer currently used for the hybrid meniscus scaffolds, p(DTD DD) was selected for evaluation. The fibers used in this study were synthesized and extruded by Dr. Joachim Kohn and Dr. Sanjeeva Murthy, (Rutgers University, Department of Biomedical Engineering, NJ Center for Biomaterials). This tyrosine-derived polyarylate has previously been used for orthopaedic tissue engineering due to its fast degradation, flexibility and elasticity provided by the aromatic backbone[40-42]. Additionally its high strength and low modulus are well adapted for environments that undergo repetitive loading. Untreated p(DTD DD) fibers (n=6) were used as the control (CO) group for this study.

2.4.1 Collagen Sponge (CS)

A collagen dispersion was created by swelling lyophilized type I, acid-insoluble bovine tendon collagen (Nitta Casings, Somerville, NJ) in an acid solution (pH 2.4) followed by homogenization in a high-speed blender. Half of this solution was used to coat the bottom of a petri dish and the p(DTD DD) fibers (n=6) were then placed on top. The remaining dispersion was used to cover the fibers and the petri dish was then frozen and lyophilized overnight in a Freezone 1L system (Labconoco, Kansas City, MO).

2.4.2 Crosslinking (EDC)

1-Ethy-3-[3-dimethylaminopropyl] carbodiimide hydrochloride (EDC), a zero order crosslinking ageny, has been used at RWJ to crosslink the fiber-reinforced collagen sponges for meniscus replacement. In accordance with this protocol, p(DTD DD) fibers (n=6) were placed in 10mM EDC and 5mM N-Hydroxysuccinimide in deionized water for 24 hours, followed by three 10-minute rinses in deionized water to remove urea, an easily removed byproduct of EDC crosslinking[43]. The fibers were then placed in a 0.1 M Na_2HPO_4 solution for 2 hours followed by four 6-hour rinses in deionized water. The fibers were then allowed to dry in a desiccator overnight before testing.

2.4.3 Freeze drying (FD)

Individual p(DTD DD) fibers (n=6) were placed in a sealed petri dish and submersed in an ethanol dry ice bath. Once frozen, the seal was removed and the dish was subjected to overnight lyophilization.

2.4.4 Sterilization (IR)

Instant sealing sterilization pouches (Fisher Scientific Inc., Pittsburgh, PA) were used to contain single fibers (n=6) during the sterilization process. In accordance with the

meniscus protocol, the pouches were exposed to 25kGy of E-beam radiation (Sterigenics, Cranberry, NJ). Upon return, the fibers were stored away from light until mechanical testing.

2.4.5 Combination Treatments

In addition to the effects produced by individual processing conditions, this study also aimed to evaluate the effect of combination treatments, including the entire process, on individual p(DTD DD fibers). Each sample group utilized combinations of the individual treatments described earlier. These were defined as (1) EDC & FD, (2) EDC, FD&IR, (3) CS, EDC, FD&IR (n=6 for each group).

2.4.6 Mechanical testing

All samples were tested using a modified version of the American Society for Testing and Materials (ASTM) D3822, Standard Test Method for Tensile Properties of Single Textile Fibers. Prior to testing, fiber diameters were measured using a laser micrometer (Z-mike model 1202B, Dayton, OH). Each end of the p(DTD DD) fiber was taped to delineate a 50 mm gauge length. Fibers were mechanically loaded until failure at a constant strain rate of 60% strain/minute using an Instron Mechanical Testing System (Norwood, MA) model 5569, with a 100N load cell and Bluehill software (Figure 2-2).

Figure 2-2: Mechanical testing of single p(DTD DD) fibers.

2.4.7 Data Analysis

A custom MATLAB script (The MathWorks Inc., Natick, MA) was used to determine the polymer fiberôs material properties from the mechanical data. Fiber diameter was calculated as the average of three measurements taken prior to testing. The youngôs modulus was defined as the maximum slope within the linear region of the stress-strain plot. A 0.2% offset yield point was used to determine the yield stress and strain. Table data is presented as mean ± standard deviation.

2.4.8 Statistical Analysis

Averages and standard deviations of the material properties were calculated for each of the seven treatment groups. An unpaired, two-tailed studentôs t-test was utilized to identify significant differences between the untreated control group and each treatment condition. A p-value of less than 0.05 was considered significant.

2.5 Results

PLLA fibers that underwent various combinations of meniscus scaffold processing techniques were subject to tensile testing and their mechanical properties were determined (Table 2-1). There were significant differences identified between each individual treatment (COL,EDC,FD,IR) and untreated p(DTD DD) fibers as well as combination treatments, with respect to material properties.

2.5.1 Individual Treatments

To better understand the influence of processing conditions on polymer mechanics, each processing step was first tested individually. Tensile testing of the PLLA fibers, with an average diameter of 0.11 mm, revealed that all individual treatments significantly decreased yield strength when compared to untreated fibers (Table 2-1:). While the addition of collagen and irradiation decreased all materials properties, freeze-drying only significantly affected the fibersô yield strength. Crosslinking decreased both yield strength and yield strain; however the change in youngôs modulus was not significant.

Table 2-1: Material properties of p(DTD DD) fibers. (CS- collagen sponge, EDC- crosslinked, FD- freeze dried, IR- irradiated). Average ± standard deviation.

	Yield Strength (MPa)	Yield Strain (%)	Young's Modulus (MPa/%)
p(DTD DD)	118.23 ± 3.56	7.32 ± 1.92	22.66 ± 2.93
CS	78.77 ± 12.06*	4.35 ± 0.46*	19.36 ± 1.16*
EDC	73.15 ± 12.03*	3.69 ± 1.29*	20.31 ± 1.97
FD	84.94 ± 22.36*	4.96 ± 2.28	20.46 ± 1.32
IR	60.48 ± 5.15*	3.43 ± 0.66*	19.29 ± 1.23*
EDC+FD	60.40 ± 2.85*	3.96 ± 0.47*	17.60 ± 0.71*
EDC+FD+IR	64.21 ± 13.17*	4.09 ± 1.62*	19.73 ± 1.47
CS+EDC+FD+IR	69.84 ± 12.51*	6.33 ± 2.97	17.04 ± 3.66*

*Statistically different from untreated p(DTD DD) ($p<0.05$) $n=5$

2.5.2 Combination Treatments

Polymer fibers were then exposed to combinations of treatments and compared with untreated fibers. These experimental groups showed that all material properties were significantly decreased when exposed to EDC and then freeze dried (Table 2-1). However, when irradiation was added, the change in the youngôs modulus was no longer notable. Finally, with the addition of collagen completing the production process, the yield strength and youngôs modulus were significantly decreased.

2.6 Discussion

These experiments addressed the first objective of this thesis: to determine the effect of scaffold processing techniques on individual polymer fiber strength. The purpose of these studies was to provide insight into the changes occurring in tissue-engineered meniscal replacements during their fabrication.

2.6.1 Collagen Sponge

In order to meet the functional demands of the native meniscus, a tissue-engineered replacement must attempt to recapitulate both the tensile and compressive properties. Our laboratory aimed to reinforce a collagen sponge, capable of opposing a compressive force, with a quasi-woven fiber pattern. The purpose of this study was to see how the addition of the collagen sponge affects the fiberôs mechanical properties.

In this study, individual p(DTD DD) fibers were placed into a collagen dispersion and freeze dried to discern the effect, if any, that it had on the polymerôs elastic properties. The addition of collagen significantly decreased the yield strength, strain, and

youngôs modulus. Therefore the injection of the collagen dispersion resulted in a smaller elastic region and reached its plastic deformation region at a much slower rate.

When collagen was included in the final combination of all the treatments, the yield strength was dramatically decreased when compared with native tissue. Additionally the youngôs modulus was also affected. However, the change in yield strain was unremarkable. This preservation of a component of the elastic limit could be due to the cross-linking of the collagen sponge, however it is unlikely, as the crosslinks should only affect the collagen dispersion and not the polymer fiber.

2.6.2 Crosslinking

A tissue-engineered resorbable meniscus replacement must meet the functional benchmarks of the native meniscus immediately after implantation. The collagen sponge developed in our laboratory is strengthened with the addition of crosslinks that affect the polymerôs initial strength and influences the degradation profile.

In this study, individual p(DTD DD) fibers were crosslinked with EDC and NHS to evaluate the effects of the treatment alone and in addition to the subsequent fabrication steps. EDC alone induced a significant decrease in yield strength and yield strain without a notable difference in the fiberôs tensile modulus. Fibers approached their elastic limit at the same rate, however the limit was appreciably smaller than untreated p(DTD DD) fibers.

This decrease in the yield strength was also seen in all combination treatments that included EDC. Additionally, when EDC and freeze-drying were combined, as well as when collagen, EDC, freeze-drying and sterilization were combined, there was a

significant decrease in the youngôs modulus, indicating a decreased fiber elasticity. However this decrease in elasticity was not observed in the EDC-FD-IR combination group preventing the identification of a causal relationship. Interestingly, when EDC-only fibers were compared to EDC-FD combination fibers using a two-tailed t-test, both the yield strength and youngôs modulus were significantly different, suggesting freeze-drying potentially wielded a larger influence on elastic properties.

2.6.3 Freeze Drying

Individual polymer fibers were lyophilized to create a freeze-dried control group for this study. This study revealed that lyophilization significantly decreased the yield strength, however it had the least impact on yield than any other treatment. Additionally it did not notably impact the yield strain or youngôs modulus of the polymer fibers. Therefore, extreme losses in the polymerôs elastic properties during combination treatments would be primarily attributed to the other conditions in the combination.

When combined with additional treatments, decreases in the elastic yield point were observed. The exceptions to this were the yield strain in the full treatment combination as well as the youngôs modulus in the EDC, FD and IR group. When both FD-only was compared to the EDC-FD collagen fibers using a two-tailed t-test, both the yield strength and youngôs modulus were significantly different, just as with EDC. This suggests the possibility of a synergistic affect when EDC and FD are combined.

2.6.4 Irradiation

Individual polymers were treated with 25kGy of e-beam irradiation to determine the effect of sterilization on polymer fiber mechanics. This study revealed the most dramatic decreases in yield strength and strain for an individual treatment. Additionally

there was also a notable decrease in the youngôs modulus. These results indicate that irradiation decreases the elastic energy and elasticity of the polymer.

When used in combination with EDC and freeze-drying, there was still an appreciable decrease in the yield stress and strain, however the youngôs modulus was no longer significantly affected. Additionally, when the collagen sponge was added into the mix, the yield strain was no longer affected but the change in youngôs modulus became significant. When EDC-FD group was compared to the EDC-FD-IR combination using a two-tailed t-test the yield strain and youngôs modulus were shown to be significantly different, an indication that sterilization could potentially be responsible for the decrease in elastic modulus. However when irradiation alone was compared to the FD-EDC-IR group the youngôs modulus was no longer significantly decreased, suggesting that EDC-FD might be responsible for the decrease in yield strain while the decrease in youngôs modulus could be attributable to sterilization. Additionally, literature has shown e-beam irradiationôs effect on polymers. While little information is available regarding p(DTD DD), there has been research done on alternative polymers for medical devices. E-beam irradiation of PLLA, a common orthopaedic polymer, showed bulk degredation[44,45]. This suggests the possibility that irradiation at 25kGy has caused degradation in the p(DTD DD) fibers used in this study.

2.6.5 Summary

The purpose of the study was to determine if the production techniques used for meniscus tissue-engineered replacements affected the scaffoldôs elastic properties. Additionally, individual and combination treatments were examined in hopes that any appreciable difference could be attributed to a specific treatment and addressed in future

generations of the implant. When the production process was carried out from start to finish, there was a dramatic loss in yield strength that was accompanied by a minimal loss in the youngôs modulus. This decrease in elastic energy could not easily be attributed to a single treatment, however the additional groups did elucidate the significant impact caused by irradiation alone and the combination of EDC and freeze-drying. It must be noted that while significant differences were found in the yield strength of all groups, all except irradiation and EDC-FD had standard deviations greater than 12. These large deviations combined with small sample size make it difficult to identify specific process that dramatically alters polymer mechanics, however global changes could be observed and may be used as the foundation for future studies.

2.7 Limitations and Future Directions

The difficulty in determining causal relationships between sample groups could be due to the relatively small sample size used for fiber testing (n=6). The sample size for this study was constrained due to the amount of polymer fiber available as well as the ability to adequately grip the single fibers during tensile testing. The large standard deviations in yield strength could be potentially avoided with an increase in sample population. A post-hoc power analysis placed all yield strengthôs at greater than 90%, and the majority of yield strainôs above 91% however the majority of the youngôs moduli had a power below 70%. Future testing should incorporate a larger sample size, evaluate different ways to grip individual fibers, as well as compare the effects of production on a different polymer such as PLLA.

CHAPTER 3: Design of a nanofibrous circumferentially-aligned collagen-PLLA composite scaffold

3.1 Rationale

The technique of electrospinning for scaffold-based tissue engineering has become increasing popular in the literature. A high voltage is applied to a polymer droplet causing it form a ñtaylor coneò that emits a charged jet. The jet is then subject to a whipping process that elongates the polymer into a fiber while traveling towards a grounded collector. While the technique originated in the textile industry during the 1930ôs, its medical uses span from drug delivery and cardiovascular stents to wound treatments. Unlike the traditional polymer extrusion techniques that produce fibers like those described in Chapter 2, electrospinning is capable of producing nanofibrous mesh-like sheets on a similar scale to components of the extracellular matrix (ECM), including collagen[46-48]. The mechanical properties of electrospun scaffolds have been shown to affect cellular infiltration, proliferation, differentiation and morphology[49,50]. These nanofibrous scaffolds have the potential to serve as a provisional ECM in orthopaedic implants aimed at regenerating native tissue. Additionally, electrospun scaffolds can be trimmed to size without destabilizing fiber alignment, unlike polymer macrofibers, which is an important feature of a potential partial meniscal replacement that could be custom fit based on defect location and size.

A prerequisite to the use of electrospinning in orthopaedic tissue engineering is its ability to produce oriented nanofibrous sheets. The preferential fiber alignment of anisotropic musculoskeletal tissues is integral to their function. In the meniscus, circumferentially aligned fibers convert femoral loads into hoop stress increasing force distribution over the tibial plateau[51-54]. This perquisite was partially fulfilled with the

production of axially, or linearly, aligned scaffolds[55,56] and fully achieved more recently with the creation of circumferentially aligned scaffolds[3](Figure 1-7).

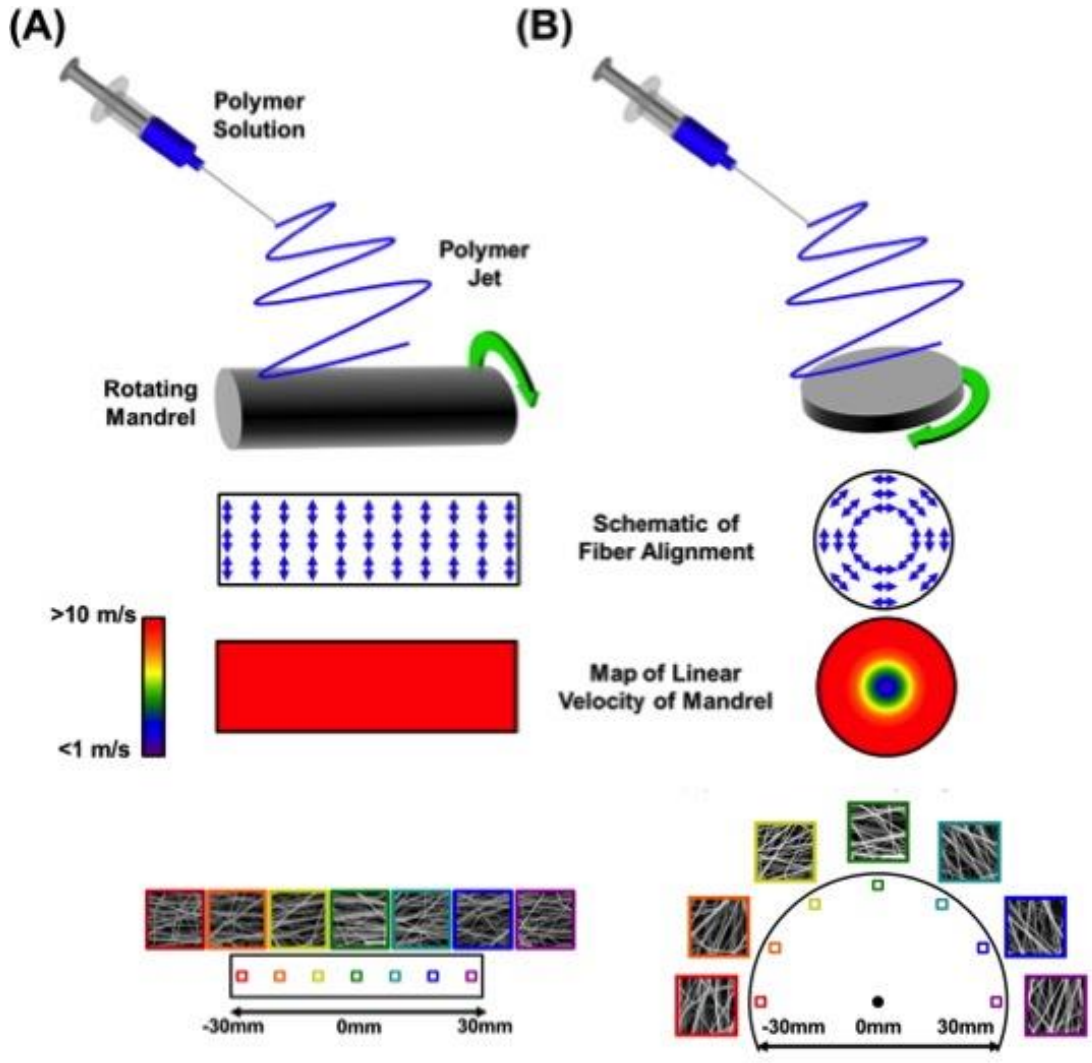

Figure 3-1: Comparison of linearly aligned and circumferentially aligned electrospun scaffolds. Figure adapted from Fisher[3].

However promising, these scaffolds only address the tensile forces of the meniscus, while the collagen fibers and proteoglycans of native meniscal tissue also provide the equally important viscoelastic component of meniscus biomechancis[52,57-59]. This property is essential to the menisciôs functionality and to the integrity of bordering

articular surfaces. Electrospinning of collagen, while possible, does not preserve native collagen structure, with the literature reporting a 57-99% loss of triple helical structure[60-62], resulting in a mechanically weak network of gelatin.

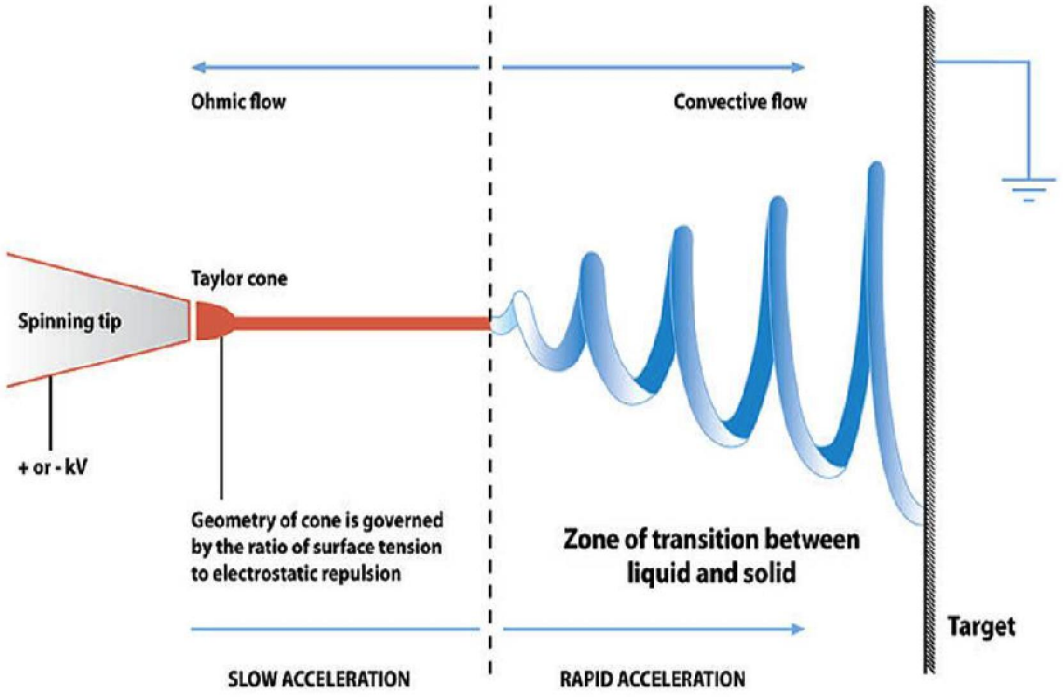

Figure 3-2: Electrospinning "Taylor cone" and whipping process. Figure adapted from Wikipedia[63].

Collagen is often incorporated into scaffolds for tissue regeneration in order to harness its functionality. However, the mechanism by which conformational changes affect these processes is widely debated in the literature. Within the extracellular matrix, collagen acts as a chemotactic agent, recruiting and stimulating cells such as fibroblasts. It has been shown that both intact collagen fibrils and collagen peptides are chemotactic[64]. Therefore it is unlikely that unfolding of the molecule during electrospinning would result in a loss of cell recruitment. Additionally, collagen serves as a matrix for cell attachment. Many of the receptors that mediate these relationships are formed out of the triple helical

structure of collagen, which is lost during electrospinning. Additional receptor sites are exposed upon unfolding, however these serve as signals for collagen turnover and peptide incorporation[65]. While conformational changes that occur during electrospinning might impair cell attachment to the collagen matrix, collagen may still retain its ability to recruit fibroblasts. This study aimed to retain the functionality of collagen, namely cell recruitment and attachment, by avoiding the structural changes associated with electrospinning.

3.2 Objective

To provide a tissue-engineered solution that recapitulates both the tensile and compressive properties of meniscal tissue on a nanoscale, this study aimed to create a nanofibrous, circumferentially aligned collagen-PLLA composite scaffold that preserved the native collagen structure as well as the mechanical integrity of nanofibrous scaffolds. To achieve this, lyophilized collagen powder was added to the scaffolds as the nanofibers collected on a rotating disc.

3.3 Hypotheses

A composite collagen and synthetic polymer scaffold can be produced that 1) preserves the tensile properties of electrospun PLLA scaffolds and 2) achieves a clinically-relevant thickness for meniscal tissue engineering.

Null Hypotheses:

- Circumferentially aligned scaffolds will have mechanical properties equal to that of linearly aligned fibers.
- The addition of collagen will not affect the mechanical properties of electrospun scaffolds.

3.4 Materials and Methods

Materials and methods were selected based upon their ability vary the architecture of electrospun sheets. The first step was to design an electrospinning set-up including a collection mandrel capable of producing circumferentially aligned fibers. The second objective was to design and mechanically evaluate a collagen-PLLA hybrid scaffold. Five samples were prepared for each of the three conditions: linearly aligned fibers, circumferentially aligned fibers, and circumferentially aligned collagen-polymer composite scaffolds.

3.4.1 Set-up for Electrospinning Process

The electrospinning setup consisted of an 18-gauge blunt-end stainless steel needle acting, as a metal spinneret, that was pushed through an aluminum rectangle connected to the positive electrode of a high voltage power supply (Gamma High Voltage Ormand Beach, FL, ES30-5W), thereby avoiding the directionality associated with a traditional alligator clip[66]. The spinneret was connected to a syringe filled with polymer solution that was then placed in a syringe pump to control the flow rate of polymer solution. The syringe pump was then oriented towards the collecting surface. Depending on the experiment, the collecting surface was grounded or placed in front of a grounded plate.

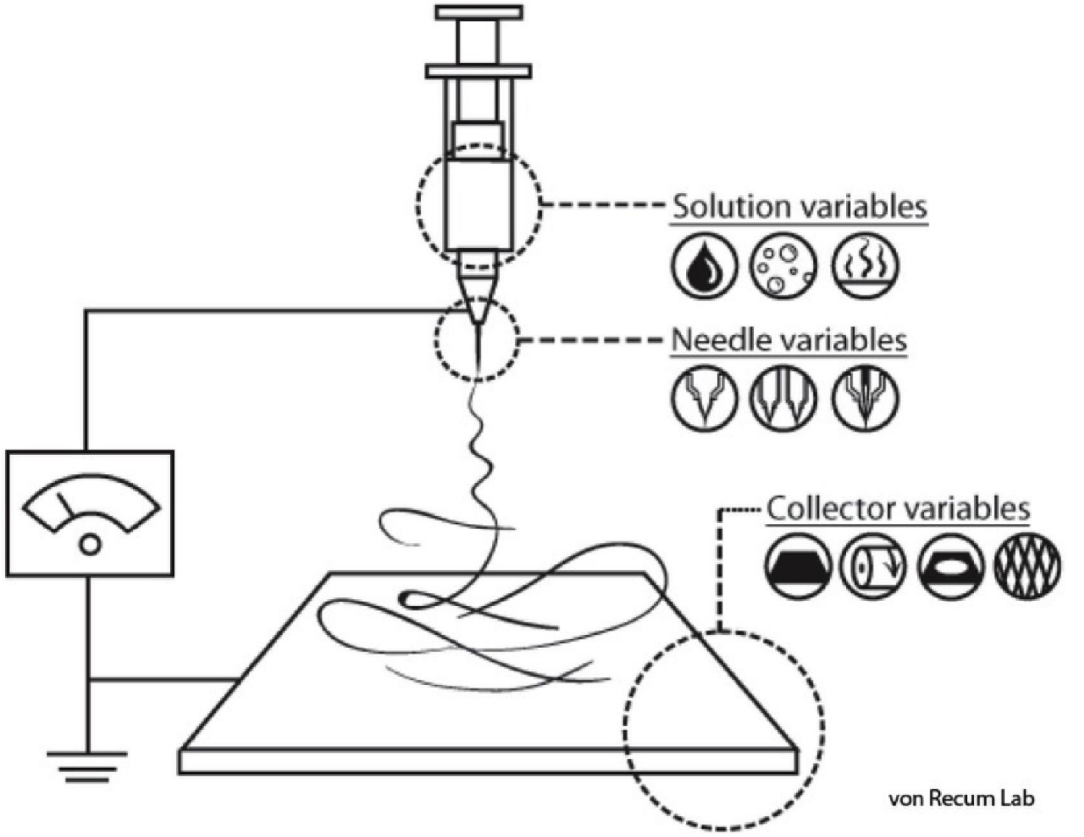

Figure 3-3: Diagram of electrospinning set up and variables that influence the fabrication process. Figure adapted from Wikipedia[63].

3.4.2 Polymer and Solvent Selection

Poly-L-lactic acid (PLLA) (PURASORB) is a well-known, FDA-approved polyarylate. It was chosen due to its ease of availability, prevalence in literature, and rapid solubility in solvents. PLLA pellets were purchased from Purac Biomaterials, Inc. (USA). Polymer concentration, one of many ways to influence the morphology of electrospun sheets, was kept consistent to determine the effect of study variables. A 7% (w/v) PLLA solution was obtained by dissolution of the polymer in 75% dichloromethane (DCM) (Sigma-Aldrich St. Louis, MO) and 25% dimethylformamide (DMF) (Sigma-Aldrich St. Louis, MO) (v/v) followed by mixing overnight.

3.4.3 Confirmation of Fiber Morphology

Glass slides measuring 75 by 25 mm were attached to the rotating collection targets and allowed to collect fibers for a period of ten seconds. The slides were visualized under a light microscope and the percentage of aligned fibers was subjectively determined. This local fiber alignment coupled with the macroscopic observation of global fiber alignment (linear vs. circumferential) provided generalized insight into scaffold morphology (Figure 3-5).

3.4.4 Linearly Aligned PLLA Scaffolds (AA PLLA)

To produce linearly aligned fibers, a syringe pump was oriented horizontally at a distance of 10 cm from the target (Figure 3-4). PLLA was electrospun onto a rotating mandrel (~2000 rpm) at a rate of 5ml/hr for a total of 5ml. A 15-20kV differential was applied using an alligator clip for the metal spinneret and a grounded aluminum plate positioned behind the collection mandrel (Box used at Dr. Freemanôs MoTR Lab, Rutgers University, Piscataway, NJ).

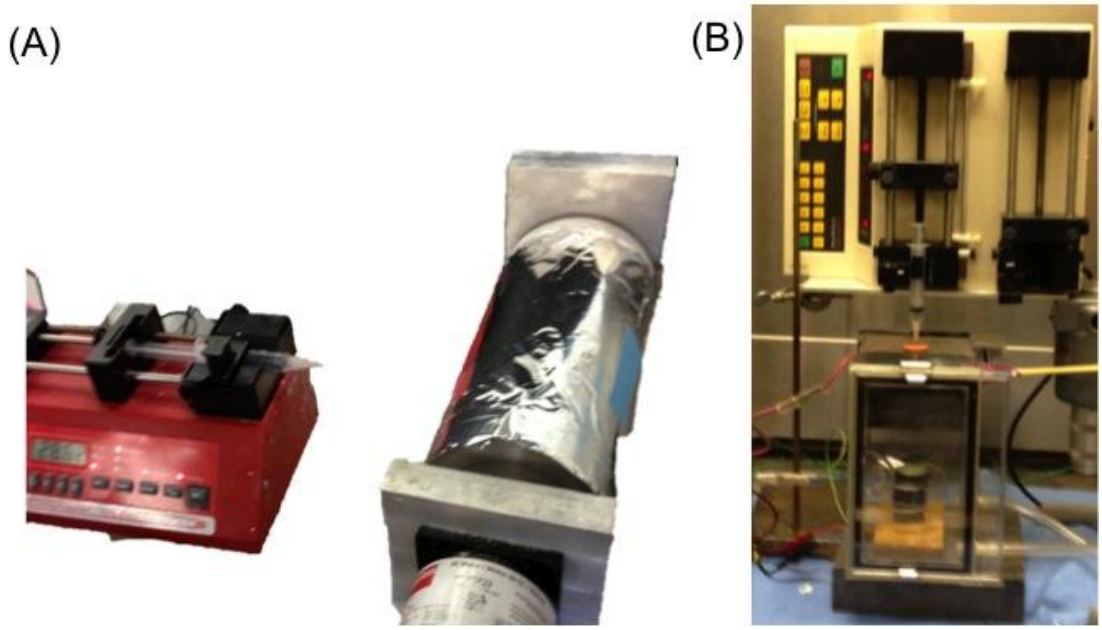

Figure 3-4: Comparison of setup for (A) linearly aligned and (B) circumferentially aligned fibers.

3.4.5 Circumferentially Aligned PLLA Scaffolds (CA PLLA)

To produce circumferentially aligned fibers a syringe pump was oriented vertically above the rotating mandrel and perpendicular to the collecting surface[3]. A rotating disc (3ò diameter fender washer) was connected to the end of the motorôs shaft. To direct circumferential alignment the ground wire was stripped to expose the encased wire and positioned to continuously contact the underside of the collection disc.

Polymer solution was dispensed at 5ml/hr and drawn out of the metal spinneret by applying a 15-20kV potential at a distance of 12 cm above the target for a total volume of 5ml. Mandrel rotation speed was controlled by motor input voltage. A range of voltages was analyzed to confirm fiber alignment (5-25V) and a subjective assessment of slide spins showed 20-25V was sufficient to produce circumferentially aligned fibers. For the

purposes of this study, mandrel rotation was set at 25V, as literature has shown the correlation between speed and alignment[3,55].

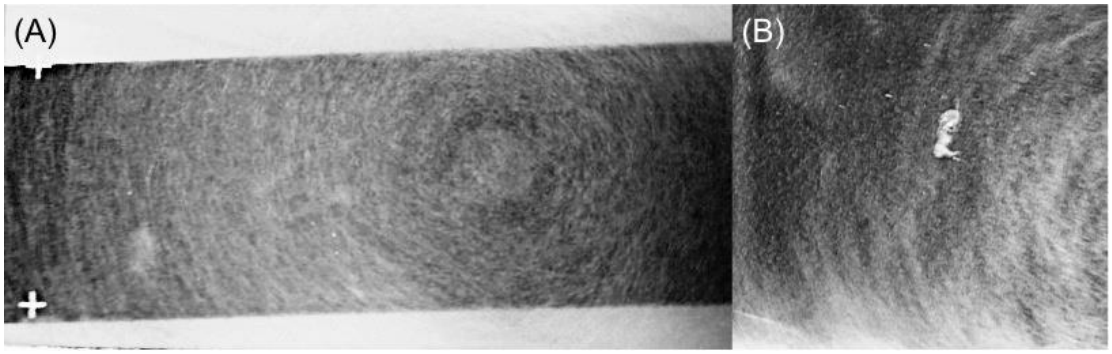

Figure 3-5: Circumferentially aligned slide spin showing the (A) global fiber orientation. (B) Additional close up view of fiber orientation. White debris (collagen) attached itself after the spinning process.

3.4.6 Collagen-PLLA Hybrid Scaffolds (CA CS-PLLA)

The setup and electrospinning parameters described in section 3.4.5 for circumferentially aligned fibers were employed for this study. Lyophilized type I, acid-insoluble bovine dermal collagen (Nitta Casings, Somerville, NJ) was ground down to a powder and weighed into shaker pods, with approximately 0.5grams/pod. The pods consisted of a plastic outer shell punctured repeatedly with an 18-guage needle in one small region, which allowed collagen powder to escape. Pods were positioned on the opposite side of the collection disc from the metal spinneret and dynamically shaken at select frequencies (0.25, 1, 2 Hz) to incorporate collagen into the growing scaffold. After spinning, collagen that did not integrate was collected and weighed. This weight was subtracted from the total weight of collagen dispensed into the pods to provide a rough estimate of collagen content of the scaffolds.

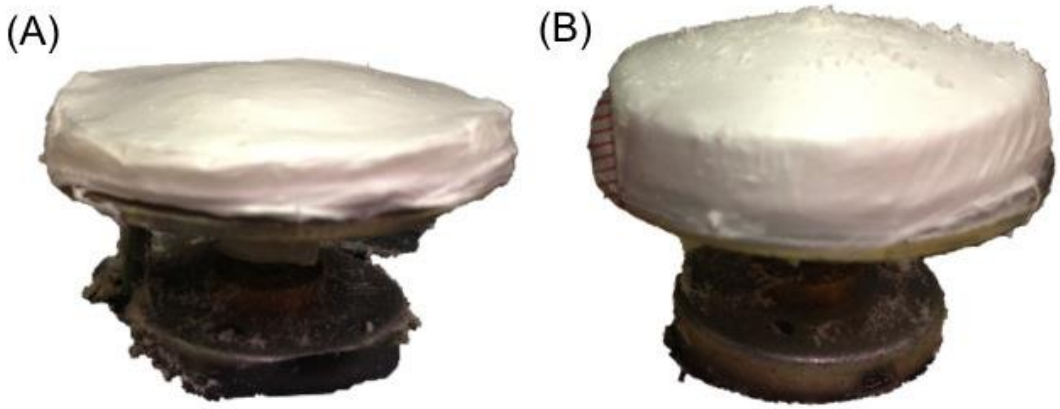

Figure 3-6: Composite collagen-PLLA scaffolds containing (A) 1Hz frequency, ~1 gram collagen and (B) 2Hz frequency, ~2 grams of collagen.

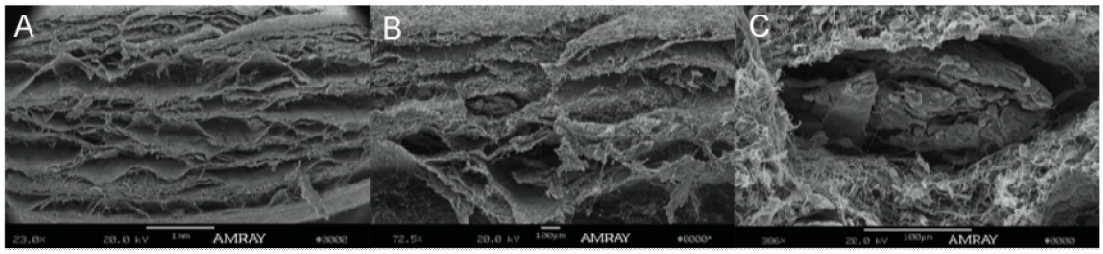

Figure 3-7: SEM image of composite scaffold. (A) 23x magnification, global view of scaffold cross-section, (B) 72.5x magnification displaying composite nature of scaffold, (C) 386x magnification displaying embedded collagen.

3.4.7 Mechanical Testing

All samples were tested using a modified version of the ASTM D6638, Standard Test Method for Tensile Properties of Plastics. Samples were prepared by removing 5 mm by 40 mm strips from electrospun scaffolds. Prior to testing, sheet thickness was measured using a laser micrometer (Z-mike model 1202B, Dayton, OH) and each end of the sample was taped to delineate a 10 mm gauge length. Samples were mechanically loaded until failure at a constant strain rate of 0.1% strain/second using an Instron

Mechanical Testing System (Norwood, MA) model 5569, with a 100N load cell and Bluehill software.

Figure 3-8: Preparation of Electrospun scaffold for mechanical testing.

3.4.8 Data Analysis

Fiber orientation was subjectively assed through microscope visualization of slide spins and used solely in the determination of mandrel speed. Sheet thickness was defined as the average of three measurements taken prior to testing, however scaffolds exceeding 5mm were assessed using a custom MATLAB image analysis script. The linear stiffness and youngôs modulus were defined as the maximum slope within the linear region of the load-deformation and stress-strain plots, respectively. A 0.2% offset yield point was used to determine the yield stress and strain. Mechanical data was analyzed using a custom MATLAB script to determine the structural and material properties of scaffolds. Table data is presented as mean ± standard deviation.

3.4.9 Statistical Analysis

Averages and standard deviations of the structural and material properties were calculated for each of the three groups. An unpaired, one-tailed studentôs t-test was utilized to identify significant differences in mechanical properties between collection mandrels as well as PLLA and collagen composite scaffolds. A p-value of less than 0.05 was considered significant.

3.5 Results

3.5.1 Failure Analysis of Fiber Aligned Scaffolds

In order to produce an electrospun meniscus scaffold, mechanical properties of linearly aligned and circumferentially aligned nanofibrous scaffolds produced on two different mandrels were compared. As seen in Table 3-1:, there was a significant increase in all structural and material properties, except for the appreciable decrease in yield strain.

Table 3-1: Structural and material properties of electrospun PLLA scaffolds. (AA- axially aligned, CA- circumferentially aligned, CA CS- circumferentially aligned collagen-PLLA hybrid). Average ± standard deviation.

	Thickness (mm)	Stiffness (N/mm)	Ultimate Load (N)	Young's Modulus (MPa/%)	Yield Strength (MPa)	Yield Strain (%)
LA PLLA	0.58 ± 0.12	1.74 ± 0.71	0.57 ± 0.14	0.07 ± 0.03	0.16 ± 0.05	7.33 ± 2.70
CA PLLA	0.90 ± 0.08*	10.92 ± 2.55*	8.86 ± 3.51*	0.49 ± 0.22*	0.74 ± 0.20*	2.88 ± 1.41*
CA CS-PLLA	3.92 ± 0.60^	10.30 ± 2.84	18.16 ± 1.56^	0.08 ± 0.01^	0.36 ± 0.18^	6.43 ± 3.67^

*Statistically different from LA PLLA (p<0.05) n=5
^Statistically different from CA PLLA (p<0.05) n=5

3.5.2 Failure Analysis of Collagen-PLLA Composite Scaffolds

To better understand the effect of native collagen incorporation on electrospun scaffolds, collagen was integrated into the fibers during the spinning process and the

mechanical properties of the construct were determined. Image analysis confirmed the drastic change in scaffold thickness observed during production. The amount of collagen incorporation was correlated with scaffold thickness, as scaffolds that incorporated roughly 0.5, 1, and 2 grams of collagen resulted in scaffolds thicknesses of approximately 2, 4, and 10 mm, respectively. Additionally, testing showed a significant increase in the ultimate load and yield strain for composite scaffolds, as well as an appreciable decrease in the youngôs modulus and yield strength when compared to non-composite constructs (Table 3-1). Scaffold stiffness was not significantly affected.

3.6 Discussion

This study aimed to produce circumferentially aligned nanofibrous PLLA scaffolds and combine this with native collagen powder in a composite scaffold. The ultimate goal was to develop a composite scaffold that could recapitulate the microenvironment and mechanical properties of the native ovine meniscus for use in a tissue engineered replacement.

3.6.1 Failure Analysis of Fiber Aligned Scaffolds

Linearly and circumferentially aligned electrospun sheets were produced on two different mandrels and mechanically tested in tension to failure. This study showed an increase in all structural and material properties, with the exception of yield strain, which decreased significantly. As the collection area of the mandrels were very different, it is not surprising that their structural properties werenôt comparable. However it does point out the efficiency of using a rotating disc target. While three-dimensional scaffolds can be produced using large sheets, the process generally entails the cutting out multiple

sheets in the shape of the scaffold and fusing them together using a variety of methods found in the literature. This method is time consuming, wastes polymer, and produces scaffolds with low shear strength. The rotating disc allows for production of thicker sheets with the same amount of polymer, which has been deposited on an appropriately sized mandrel.

3.6.2 Failure Analysis of Collagen-PLLA Composite Scaffolds

Collagen was introduced into the circumferentially aligned scaffolds to determine the affect it would have on the constructôs mechanical properties. This study showed that while the addition of collagen greatly increased the thickness and ultimate load of electrospun scaffolds, the youngôs modulus and yield strength decreased appreciably. Yield strain was also found to significantly increase. These differences could be attributed to the disruption of the electrospun network. As nanofibers are deposited onto the mandrel, the collagen powder disrupts the contact between fibers. While we aimed to preserve the scaffolds material properties despite the addition of collagen, the data reveals that the alternative hypothesis was true and collagen did affect the constructs material properties.

While initially discouraging, the significance of this study is two fold. First, it demonstrated the ability to create a scaffold of clinically relevant thickness that incorporated collagen in its native orientation. Electrospinning has been used to design sheets, tubes and thin scaffolds for medical use, however the ability to create large three-dimensional scaffold with mechanical integrity is difficult. Here we present a scaffold of significant thickness, prior to any mechanical or chemical expansion. Secondly, we were able to show a relationship between the amounts of collagen incorporated and scaffold

thickness. This provides a method to balance the size of scaffolds with the loss of initial mechanical properties. Despite a decrease in material properties, this composite scaffold shows initial promise for tissue-engineered meniscus scaffolds. It is possible that future designs could incorporate post-processing techniques to increase the mechanical properties of these scaffolds.

3.7 Limitations and Future Directions

As with the start of any new production technique, this study had several limitations including processing variables and collagen incorporation. A fixed polymer concentration of 7% PLLA was used so that conclusions could be drawn regarding alternate processing variables. However electrospinning solutions can range from 4-13% with varying success. As polymer concentration increases so does fiber diameter. By altering polymer concentration you can control the structure of the microenvironment. Additionally, you can also manipulate fiber morphology by decreasing the rate at which polymer is dispensed (0.5-5 ml/hr) and varying the applied voltage, which influences the size of nanofibers[67-72]. In the future design of an electrospinning setup the speed settings of the collection mandrel should be readily available as there is a wealth of literature for which to correlation alignment data. All of these conditions can be altered to obtain the optimal composite scaffold for meniscus tissue engineering.

Additionally, future studies are warranted to evaluate the nature of collagen incorporation within the composite scaffold. First, the design of a user-independent process for collagen incorporation is warranted. Secondly, while we visually confirmed that collagen had been entrapped, little is known about how strongly it is held within the

matrix and whether this would affect the collagenôs swelling capacity. Pilot studies in our lab have shown the ability to swell the incorporated collagen and future studies aim to crosslink the swollen collagen in order to increase the constructs mechanical properties.

It is also possible that electrospinning technology could be used to recapitulate the 3 major types of collagen orientation for the meniscus: circumferential, radial, and unorganized superficial meshwork. A scaffold could be transferred between collectors to create several different matrix organizations mimicking the native menisciôs architecture.

CHAPTER 4: Meniscus fixation in a preclinical model: implications for tissue engineered scaffold design

4.1 Rationale

The efficacy of meniscal replacements, whether donor or tissue-engineered, depends on adequate fixation to the bone. While most literature focuses on the meniscal body, recent research has shown the importance of the meniscal root[54,73,74]. Tissue engineering of the soft tissue to bone interface is a very active field yet the meniscus to bone interface is rarely discussed. A literature search revealed only two papers a year were published regarding the meniscal roots until 2008 when Allaire found a root tear to be biomechanically equivalent to a medial meniscectomy. In the five years following this paper, 80 articles were published, with 23 papers in 2012 alone.

While meniscal attachments have recently been characterized in humans and bovine[5,73,75-82], little is known about the mechanical properties of the ovine meniscal attachments. For a tissue-engineered meniscal replacement to become a clinical reality its efficacy and long-term safety must be validated in a translational animal model. The ovine model is one of the most commonly used preclinical models for meniscal research[83,84] as their menisci posses similar mechanical properties and tibial plateau contract stresses to that of humans[85]. However the lack of comparative research on ovine and human meniscal attachments leaves the potential for fixation failure during testing in a large animal model. By approximating the strength of ovine meniscal roots, meniscus replacements will have a greater chance of reaching the clinical market.

4.2 Objective

This study aimed to provide fixation criteria for meniscus repairs and replacements in a translational animal model by characterizing the ovine medial meniscus attachments. Meniscal entheses were subject to mechanical evaluation in order to determine their strongest loading axis, differentiate between the attachment transition zones, and elucidate their time dependent and failure properties.

4.3 Hypotheses

The posterior attachment of the ovine medial meniscus will exhibit 1) superior tensile properties when tested parallel to the tibial plateau and 2) mechanical continuity with the meniscal body.

Null Hypotheses:

- The application of tensile force perpendicular to the tibial plateau will not affect the strength of the meniscal root.
- There is no mechanical difference between the meniscus-to-root transition and the root-to-bone transition of the ovine meniscal attachements.
- The mechanical properties of the medial posterior root will not differ significantly from those of the medial anterior root.

4.4 Materials and Methods

This study aimed to determine the medial meniscus fixation criteria in an ovine model to improve the strength of implants and repairs. An initial experiment was

performed to determine the appropriate direction in which to apply a tensile force for meniscal root testing. Next, a mechanical characterization of the medial posterior root transition regions, consisting of meniscus-to-root attachment and root-to-bone attachment was performed. Medial Posterior attachments were also subject to stress relaxation and creep testing in order to determine their time dependent mechanical properties. The final objective was to determine the failure strength of the medial meniscus attachments.

4.4.1 Harvest

Menisci from skeletally mature Columbian x Rambouillet sheep were harvested for this study. Frozen sheep hind limbs were obtained from the Surgical Research Laboratory at Colorado State University (Fort Collins, CO). The medial meniscus was the primary focus of this study as it is the most commonly injured meniscus, with root tears occurring more frequently at the posterior attachment[8,86].

Initial studies harvested menisci by disarticulating the tibia from the femur and removing the proximal two-thirds of the tibia, with the menisci still attached. For the stress relaxation, creep, and later failure studies utilizing bone blocks, the medial meniscus was bisected through the central region after disarticulation. Removal of meniscus-containing bone blocks was performed with a bone saw. All menisci were wrapped in saline soaked gauze and placed in the -20 °C freezer until testing.

4.4.2 Force Orientation for Mechanical Testing

Proximal tibias were cleaned and trimmed to fit in a custom designed testing jig previously developed for knee joint mechanics (Figure 4-3 a,b). Bone sections were potted with methyl methacrylate and mounted onto the Instron #5569 once dry. Samples were mounted either vertically or horizontally in reference to the orientation of the tibial

shaft. Menisci subject to vertical testing exhibited forces perpendicular to the tibial plateau while horizontal testing produced tensile forces parallel to the tibial plateau, similar to the anatomic direction of force. After the samples were locked in their proper orientation, careful dissection of the tissue around the medial meniscus was done to only leave the posterior root attached. For horizontal testing, a portion of the tibial plateau was removed to allow the grips access to the meniscus. The anterior portion of the meniscus was gripped using cryogenic freeze clamps (Enduratec, Eden Prairie, MN) with a 15 mm gauge length measure from the bony insertion of the root to the grip. Utilizing a 10kN load cell, preconditioning was carried out for 10 cycles at 10mm/min between 0% and 3% of the gauge length. Samples were then pulled to failure at a constant strain rate.

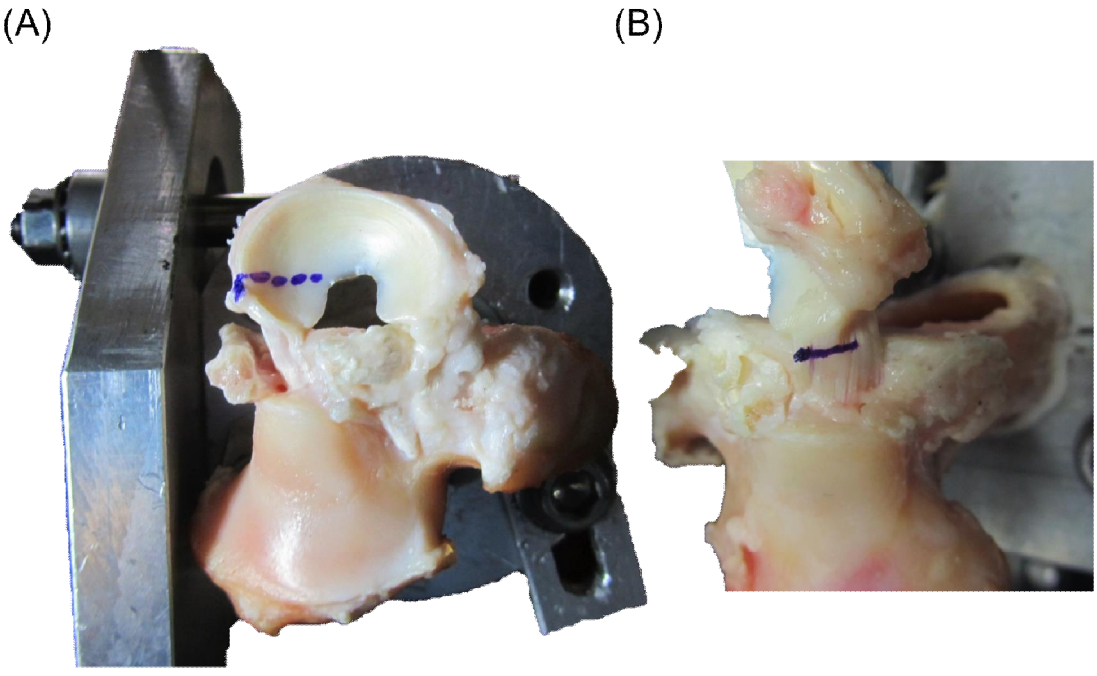

Figure 4-1: Sample preparation for horizontal testing. (A) Blue line delineates a 15 mm distance from the root insertion (guage length). (B) Tibial platuea and distal shaft was removed to allow for grips to access the posterior meniscal attachment. Blue line delineates a 4 mm distance from insertion.

4.4.3 Transition Zones

Midsubstance failures from the previous study were hypothesized to be failures located at the transition zone between the meniscal body and the root, as no failures resulted in avulsion of root tissue from the bone. In order to confirm this hypothesis, additional horizontal samples were prepared and retested using the same protocol from the previous study with the exception of a 4mm gauge length. This length consistently fell within the root and isolated testing to the tissue of the root-to-bone transition zone. However, this new method exceeded the load limits of the tibial shaft. The orientation caused the tibia to experience high torques, similar to a lever arm, and caused failure of the bone in the tibial shaft.

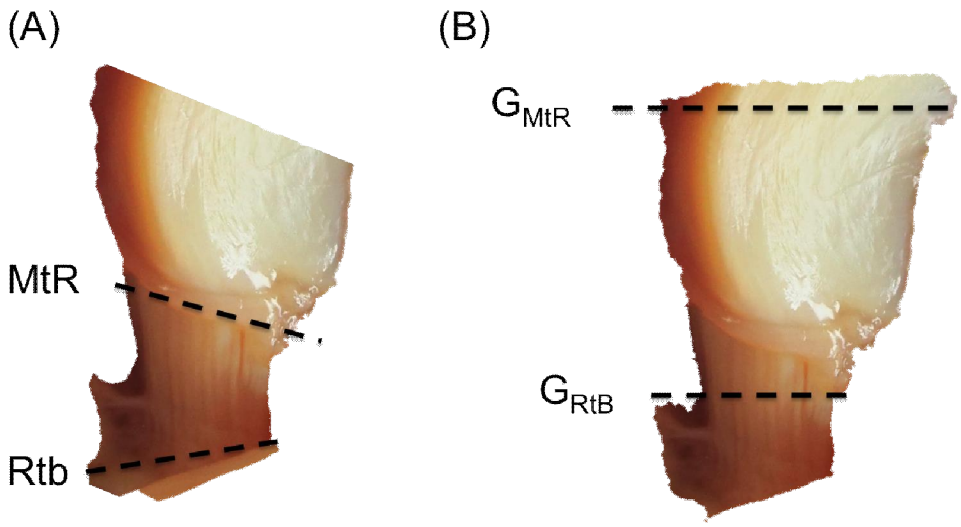

Figure 4-2: Meniscal root transition zones. (A) Meniscus body-to-root (MtR) and root-to-bone (RtB) zones. (B) Dashed lines indicate where meniscus was gripped for mechanical testing. G_{MtR} is 15 mm from insertion while G_{RtB} is 4mm from insertions.

Additional samples were tested by removal of bone blocks from the tibial plateau as described earlier. Bone blocks were oriented so the anatomical axis of the meniscal root was positioned vertically and fixed in metal pots using methyl methacrylate. Once dry, these pots were mounted onto the Instron and the meniscus was once again gripped using the cyro-clamps and tested in accordance with the previous protocol. Crosshead speed was adjusted to maintain a consistent strain rate at this new gauge length using the equation:

$$\text{[illegible]} = \frac{\text{[illegible]}}{\text{[illegible]}}$$

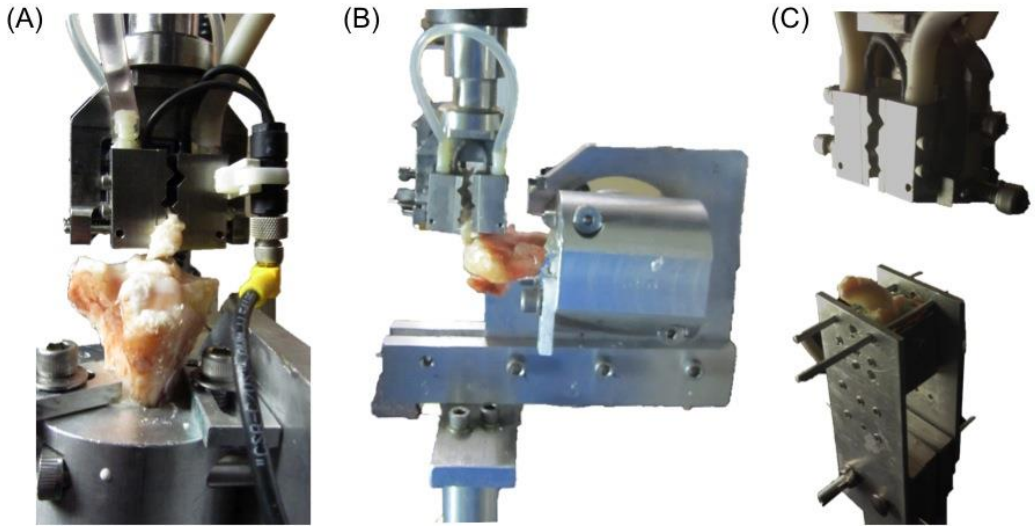

Figure 4-3: Mechanical testing of failure properties. (A) Vertical (B) Horizontal and (C) Horizontal "anatomical" testing of bone blocks.

4.4.4 Geometry

Cross sectional area was determined using a non-destructive technique originally developed for tendons and other irregularly shaped tissue and recently used for the meniscus[5,87]. Meniscal roots were surrounded with alginate impression material (Jeltrate,

Dentsply Caulk, Arnold-Dental Lynnwood, WA) and carefully removed once the meniscal impression had set (Figure 4-4). The impression material was then cut to produce a thin slice containing the outline of the meniscal root. A photograph was taken of the slice alongside a reference length and analyzed using a custom MATLAB image analysis program. The cross-sectional area of the root could be calculated without damaging the tissue, which would prevent further mechanical testing. Root lengths were measured with a micrometer in three separate regions, inner, middle, and outer to determine the average length of the entheses.

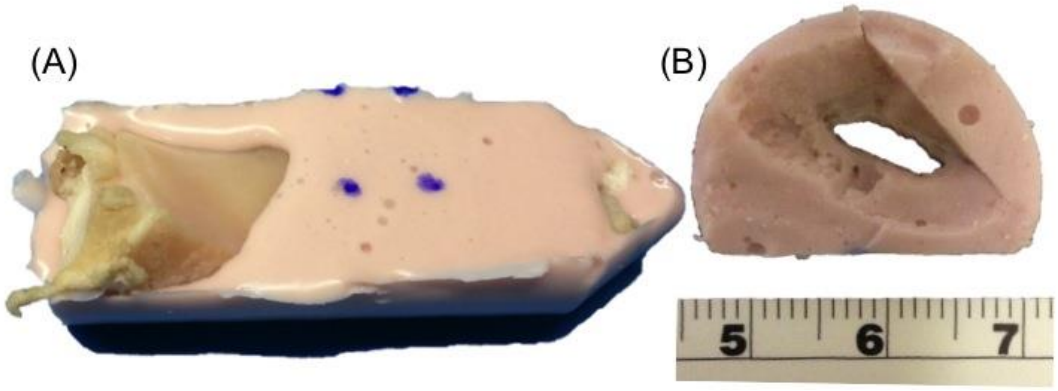

Figure 4-4: Non-destructive method to obtain quantitative cross-sectional area of irregularly shaped tissues. (A) Casting method. (B) Photo of slice for image analysis.

4.4.5 Stress Relaxation Characterization

In order to determine subfailure time dependent properties, bone blocks containing the medial posterior meniscus were fixed in acrylic pots using epoxy and allowed to dry overnight at 4 °C. Pots were then mounted into a basin that was filled with phosphate-buffered saline (PBS, pH 7.4, 37°C) and secured onto the Instron fitted with a 100N load cell. Menisci were gripped using a 4mm gauge length and samples were

preconditioned for 10 cycles at 10mm/min between 0% and 3% of their gauge length (0-0.12mm). The menisci were then ramped to a deformation of 3% of the gauge length (0.12mm) in 0.5 seconds and the deformation was held constant for 45 minutes[5,82]. Samples were then allowed to recover at 4 ℃ for 24 hours.

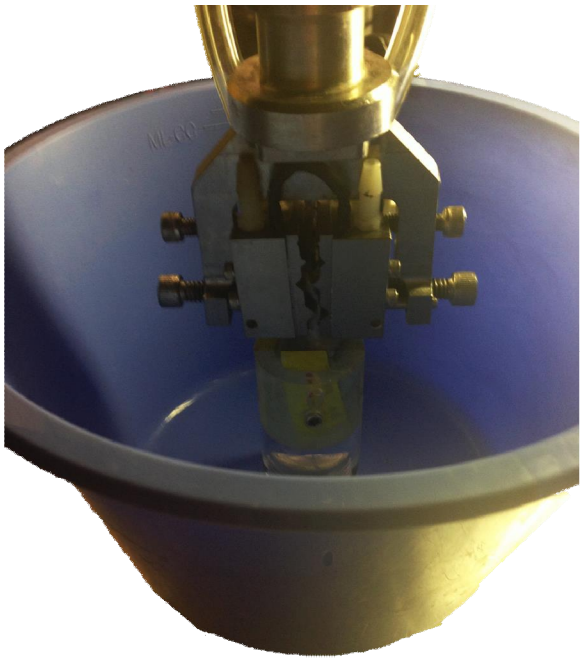

Figure 4-5: Testing set-up for time dependent properties. Basin filled with phosphate buffered saline (pH 7.4, 37°C)

4.4.6 Creep Characterization

Constant load, or creep, testing was carried out on samples that previously underwent stress relaxation testing ~24 hours earlier. The pots were mounted into the same basin filled with PBS (pH 7.4, 37°C) used in the previous stress-relaxation experiment and mounted onto the Instron fitted with a 100N load cell. The menisci were gripped using a 4mm gauge length and preconditioned for 10 cycles at 10mm/min between 0% and 3% of their gauge length (0-0.12mm). Following these precycles,

menisci were ramped up to the peak load measured during stress-relaxation testing in 0.5 seconds and held constant for 45 minutes. Samples were then allowed to recover at 4 °C for 24 hours.

4.4.7 Failure Properties: Anterior and Posterior Roots of Medial Meniscus

Posterior root bone blocks used in subfailure time dependent testing were removed from the acrylic pots and repotted in the metal pots previously mentioned. Additional bone blocks containing the anterior root were also prepared. Samples were mounted on the Instron and tested using a 10kN load cell. Meniscal roots were gripped at a 4 mm gauge length and preconditioning was performed for 10 cycles at 10 mm/min between 0-3% of the gauge length (0-0.12 mm). Finally, samples were pulled to failure at a constant strain rate.

4.4.8 Data Analysis

A custom MATLAB script (The MathWorks Inc., Natick, MA) was used to determine structural and material properties from the mechanical data. The stress relaxation and creep rates were defined as the slope of the linear region when plotted against the natural log of time and determined using linear regression. The linear stiffness and linear modulus were defined as the slope of the linear region of the load versus displacement stress versus strain plots, respectively, and calculated using linear regression. Table data is presented as mean ± standard deviation.

4.4.9 Statistical Analysis

Averages and standard deviations of the material and structural properties were calculated for the groups undergoing comparison analysis. An unpaired studentôs t-test was utilized to identify significant differences between study conditions. The force

directionality study was analyzed using one-tail, while the transition zone and anterior-posterior root comparison were conducted with two tails. A p-value of less than 0.05 was considered significant.

4.5 Results

4.5.1 Influence of Force Orientation: Posterior Root of Medial Meniscus

In order to determine the best angle to test the attachments, menisci were tested in both a parallel and perpendicular fashion, with respect to the tibial plateau. The parallel orientation may also be thought of as the anatomic orientation of native menisci. Testing revealed that the anatomic direction resulted in a significantly higher ultimate load and linear stiffness (Table 4-1). Force directionality did not appreciably affect the ultimate elongation or ultimate strain experience by the menisci.

Table 4-1: Structural and material properties of ovine medial posterior meniscus attachment obtained from load-to-failure tests. (Parallel and Perpendicular are the direction of tension in reference to tibial plateau). Average ± standard deviation.

	Ultimate Elongation (mm)	Ultimate Load (N)	Linear Stiffness (N/mm)	Linear Modulus (MPa)	Ultimate Strain (%)	Ultimate Stress (MPa)
Perpendicular	9.97 ± 2.75	386.30 ± 29.80	92.41 ± 18.22		66.48 ± 18.33	
Parallel/Anatomical	11.08 ± 3.80	696.14 ± 143.12*	127.64 ± 32.69*	125.68 ± 56.86	73.89 ± 25.33	36.07 ± 2.03

*Statistically different from perpendicular ($p<0.05$). Subfailure: nPe=4, nPa=7. Failure: nPe=4, nPa=5.

4.5.2 Transition Regions: Posterior Root of Medial Meniscus

Menisci were tested at various gauge lengths in order to determine the existence of ñtransition zonesò. When compared to gripping the meniscal body, the meniscal root-to-bone attachment had a significantly greater ultimate elongation, load and stiffness (Table 4-2). Additionally, when adjusted for size, the bony attachment had a significantly

greater ultimate strain than the meniscal body-to-root zone. However, the linear modulus was not appreciably affected.

Table 4-2: Structural and material properties of ovine medial posterior meniscus attachment transition zones obtained from load-to-failure tests. (MtR- meniscus-root, RtB- root-bone). Average ± standard deviation.

	Ultimate Elongation (mm)	Ultimate Load (N)	Linear Stiffness (N/mm)	Linear Modulus (MPa)	Ultimate Strain (%)	Ultimate Stress (MPa)
MtR	11.08 ± 3.80	696.14 ± 143.12	127.64 ± 32.69	125.68 ± 56.86	73.89 ± 25.33	36.07 ± 2.03
RtB	6.37 ± 2.03*	1091.49 ± 158.59*	275.89 ± 65.84*	87.20 ± 57.77	159.24 ± 50.64*	77.48 ± 62.99

*Statistically different from MtR ($p<0.05$) Subfailure: nMtR=7, nMRtB=11. Failure: nMtR=5, nRtB=6.

4.5.3 Geometry and Time Dependent Properties: Posterior Root of Medial Meniscus

Prior to testing, dimensional measurements were taken of the attachments and their average and standard deviation is reported in table 4-3. The menisci were then subject to mechanical testing for time dependent properties. The averages and standard deviations for the stress-relaxation (Table 4-4) and creep (Table 4-5) tests are reported below.

Table 4-3: Dimensional properties of ovine medial posterior meniscal attachment. Average ± standard deviation. n=5

	Lengths			Widths	
Cross-sectional area (mm^2)	Inner (mm)	Middle (mm)	Outer (mm)	Meniscal Edge (mm)	Insertion Edge (mm)
17.28 ± 8.76	6.77 ± 0.75	7.20 ± 0.26	10.03 ± 1.90	7.82 ± 1.75	9.23 ± 0.64

Table 4-4: Stress relaxation properties of ovine medial posterior meniscal attachment. Average ± standard deviation. n=5

				Normalized Properties			
Load at End (N)	Load Relaxation Rate (N/ln(s))	Stress at End (MPa)	Stress Relaxation Rate (MPa/ln(s))	Load at End	Load Relaxation Rate (1/ln(s))	Stress at End	Stress Relaxation Rate (1/ln(s))
0.40 ± 0.99	-0.36 ± 0.13	0.02 ± 0.07	-0.03 ± 0.02	0.06 ± 0.34	-0.16 ± 0.08	0.06 ± 0.34	-0.16 ± 0.08

Table 4-5: Creep properties of ovine medial posterior meniscal attachment. Average ± standard deviation. n=5

				Normalized Properties			
Displacement at End (mm)	Displacement Creep Rate (mm/ln(s))	Strain at End (%)	Strain Creep Rate (%/ln(s))	Displacement at End	Displacement Creep Rate (1/ln(s))	Strain at End	Strain Creep Rate (1/ln(s))
0.56 ± 0.16	0.10 ± 0.10	14.01 ± 4.05	2.38 ± 2.38	1.46 ± 0.68	0.30 ± 0.33	1.46 ± 0.68	0.30 ± 0.33

4.5.4 Failure Properties: Anterior and Posterior Roots of Medial Meniscus

On the third day of testing posterior attachment samples were subject to failure testing to determine their structural and mechanical properties. Additionally, a group of medial anterior attachments were also tested for comparison. Testing revealed no significant differences in ultimate elongation, load, or stiffness (Table 4-6). When adjusted for size, there were still no appreciable differences between the attachments.

Table 4-6: Structural and material properties of ovine meniscal attachments obtained from load-to-failure tests. (MA- medial anterior, MP- medial posterior). Average ± standard deviation.

	Ultimate Elongation (mm)	Ultimate Load (N)	Linear Stiffness (N/mm)	Linear Modulus (MPa)	Ultimate Strain (%)	Ultimate Stress (MPa)
MA	6.86 ± 2.58	940.01 ± 166.39	228.49 ± 47.75		171.39 ± 64.55	
MP	6.37 ± 2.03	1091.49 ± 158.59	275.89 ± 65.84	87.20 ± 57.77	159.24 ± 50.64	77.48 ± 62.99

No significant differences present ($p<0.05$) Subfailure: nMA=5, nMP=11. Failure: nMA=4, nMP=6.

4.6 Discussion

These experiments aimed to characterize the geometry and mechanical properties of the ovine meniscal root. The purpose of this study was to provide insight into functional benchmarks for implant fixation in a large animal model used in preclinical testing.

4.6.1 Influence of Force Orientation: Posterior Root of Medial Meniscus

In order to characterize the ovine meniscus, a mechanical testing protocol had to be developed. Initially, ease of access resulted in the meniscal root being tested in the vertical position, perpendicular to the tibial plateau. This positioning avoided any interference between the grips and the tibial plateau as well the lever arm associated with horizontal testing. However, during testing the fibers of the meniscal root were angled, resulting in an unequal distribution of tension. Fibers that were ñbentò and not in tension would only bear load once the fibers in tension failed. To compare a parallel force orientation, the tibial plateau was rotated horizontally place the menisci in an anatomical position and trimmed to allow for grip access. This orientation placed all of the attachment fibers in tension resulting in such high strengths that failures occurred at the resected bone. Once the bone block methodology was adopted, the anatomical testing of meniscal roots revealed significantly greater stiffness as well as break load when compared to perpendicular testing. This study determined that the anatomic orientation of meniscal entheses allows for tension to be distributed among the fibers and results in a more functional approximation of the attachmentôs mechanical strength.

4.6.2 Transition Regions: Posterior Root of Medial Meniscus

This study additionally aimed to determine the mechanical relationship between the meniscal body, attachment, and bony insertion. The menisci were gripped at the body or root and pulled to failure at a constant strain rate. Mechanical testing revealed a significant difference in ultimate elongation, ultimate load and linear stiffness. These results elucidated the high strength of the meniscus-to-bone attachment relative to the transition region between meniscal body and root. This high strength is necessary to

anchor the meniscus and develop the hoop stresses characteristic of this anisotropic tissue.

4.6.3 Geometry and Time Dependent Properties: Posterior Root of Medial Meniscus

In addition to failure properties, the medial posterior rootôs time dependent properties were also characterized. The average cross-sectional area of the ovine meniscal root (17.28 ± 8.76 mm^2) was much smaller than that of the human (30.70 ± 7.7 mm^2)[5] or bovine (66.5 ± 5.7 mm^2)[82]. However the length of the central region of the ovine root (7.2 ± 0.26 mm) was comparable to that of the human (7.17 ± 2.55)[5] and smaller than the bovine (between 10.0-16.3 mm)[82].

Stress relaxation analysis resulted in similarities to the bovine meniscus, as reported in the literature. The normalized load relaxation rates for ovine (-0.16 ± 0.08 1/ln(s)) and bovine (-0.136 ± 0.014 1/ln(s))[5] menisci were comparable as well as the stress relaxation rates, however they were both dissimilar from human meniscal attachments. Creep analysis revealed much higher strain creep rates for ovine meniscal attachments as compared to that of the human and bovine. For the majority of other values the ovine root fell in between the human and bovine. However the normalized displacement creep rate was similar between the ovine (0.30 ± 0.33) and the bovine (0.471 ± 0.096) root. These studies revealed significant differences between the ovine, and human attachments that could influence functional implant behavior at subfailure loads. This suggests that the size and biomechanics of preclinical models must be taken into account when designing and implant for trials.

4.6.4 Failure Properties: Anterior and Posterior Roots of Medial Meniscus

The failure properties of both medial anterior and posterior attachments were characterized and compared in order to determine the fixation benchmarks that implants must meet for successful functionality in a preclinical model. Just as in the human meniscal attachments, no significant differences were found between the anterior and posterior attachments of the ovine medial meniscus. However the ovine entheses had greater ultimate loads anteriorly (940.1 ± 166.39 N) and posteriorly (1091.49 ± 158.59 N) than humans anteriorly (455.5 ± 181.9 N) and posteriorly (591.6 ± 200.3 N)[5]. They also experienced greater elongation anteriorly (6.86 ± 2.58 mm) and posteriorly (6.37 ± 2.03 mm) than human attachments anteriorly (3.205 ± 1.246 mm) and posteriorly (2.954 ± 0.425 mm)[5]. However the ovine linear stiffness anteriorly (198.85 ±55.66) and posteriorly (264.42 ± 70.12) was comparable to that of the humanôs anteriorly (169.4 ± 24.19 N/mm) and posteriorly (207.2 ± 52.79 N/mm)[5]. While the human and ovine meniscal attachments are similar in stiffness, the ovine meniscus must ultimately withstand much higher failure loads, an important benchmark for tissue-engineered menisci to meet for success in preclinical testing prior to FDA approval.

4.7 Limitations & Future Directions

While this study finds differences in time dependent mechanical properties between ovine, bovine, and human attachments, it is unknown how these distinctions affect the functional behavior of the knee joint. The results also elucidated the weaker relationship between meniscus and root as compared to the root to bone connection, however as root avulsions occur clinically, more research is needed to evaluate these

zones in the human menisci and their role in the pathophysiology of root avulsions. It has been noted that the visual transition from meniscal body to root is much more distinctive in the ovine than in human, with a distinct overhang of meniscal body on either side of the slightly narrower root. It is possible that this overhang, within the transition region, creates a mechanically weak point in the attachment or that the collagen fibers of the root are not completely continuous with the meniscal body. However as this is pure speculation, future studies are needed to evaluate the continuity of the meniscal root and body and how it compares to humans. This information is vital for the design of tissue-engineered menisci. Fixation strength is key to an implants success and should aim to be replicated when designing a replacement for use in a preclinical model.

Resources

1. Walker PS, Erkman MJ. The role of the menisci in force transmission across the knee. *Clin Orthop Relat Res.* 1975(109):184-192.
2. Ghosh P, Taylor TKF. THE KNEE-JOINT MENISCUS - A FIBROCARTILAGE OF SOME DISTINCTION. *Clinical Orthopaedics and Related Research.* 1987(224):52-63.
3. Fisher MB, Henning EA, Soegaard N, Esterhai JL, Mauck RL. Organized nanofibrous scaffolds that mimic the macroscopic and microscopic architecture of the knee meniscus. *Acta Biomaterialia.* 2013;9(1):4496-4504.
4. Sweigart MA, Athanasiou KA. Toward tissue engineering of the knee meniscus. *Tissue Eng.* 2001;7(2):111-129.
5. Hauch KN, Villegas DF, Donahue TLH. Geometry, time-dependent and failure properties of human meniscal attachments. *Journal of Biomechanics.* 2010;43(3):463-468.
6. Arnoczky SP. Cruciate Ligament Rupture and Associated Injuries. In: Newton CD, Nunamaker DM, eds. *Textbook of Small Animal Orthopaedics*: J.B. Lippincott Company; 1985.
7. Killian ML, Lepinski NM, Haut RC, Donahue TLH. Regional and Zonal Histo-Morphological Characteristics of the Lapine Menisci. *Anatomical Record-Advances in Integrative Anatomy and Evolutionary Biology.* 2010;293(12):1991-2000.
8. Miller MD, Thompson SR, Hart J. *Review of Orthopaedics.* 6 ed. Philadelphia: Elsevier Saunders; 2012.
9. Aspden RM, Yarker YE, Hukins DWL. COLLAGEN ORIENTATIONS IN THE MENISCUS OF THE KNEE-JOINT. *Journal of Anatomy.* 1985;140(MAY):371-380.
10. Bullough PG, Munuera L, Murphy J, Weinstein AM. The strength of the menisci of the knee as it relates to their fine structure. *J Bone Joint Surg Br.* 1970;52(3):564-567.
11. Kawamura S, Lotito K, Rodeo SA. Biomechanics and healing response of the meniscus. *Operative Techniques in Sports Medicine.* 2003;11(2):68-76.
12. Garrett WE, Swiontkowski MF, Weinstein JN, et al. American board of orthopaedic surgery practice of the orthopaedic surgeon: Part-II, certification examination case mix. *Journal of Bone and Joint Surgery-American Volume.* 2006;88A(3):660-667.
13. Berthiaume MJ, Raynauld JP, Martel-Pelletier J, et al. Meniscal tear and extrusion are strongly associated with progression of symptomatic knee

osteoarthritis as assessed by quantitative magnetic resonance imaging. *Annals of the Rheumatic Diseases.* 2005;64(4):556-563.

14. Adams JG, McAlindon T, Dimasi M, Carey J, Eustace S. Contribution of meniscal extrusion and cartilage loss to joint space narrowing in osteoarthritis. *Clinical Radiology.* 1999;54(8):502-506.

15. Englund M, Lohmander LS. Risk factors for symptomatic knee osteoarthritis fifteen to twenty-two years after meniscectomy. *Arthritis and Rheumatism.* 2004;50(9):2811-2819.

16. Englund M, Guermazi A, Lohmander LS. The Meniscus in Knee Osteoarthritis. *Rheumatic Disease Clinics of North America.* 2009;35(3):579-+.

17. Allaire R, Muriuki M, Gilbertson L, Harner CD. Biomechanical consequences of a tear of the posterior root of the medial meniscus. *Journal of Bone and Joint Surgery-American Volume.* 2008;90A(9):1922-1931.

18. Bao HRC, Zhu D, Gong H, Gu GS. The effect of complete radial lateral meniscus posterior root tear on the knee contact mechanics: a finite element analysis. *Journal of Orthopaedic Science.* 2013;18(2):256-263.

19. Bedi A, Kelly NH, Baad M, et al. Dynamic Contact Mechanics of the Medial Meniscus as a Function of Radial Tear, Repair, and Partial Meniscectomy. *Journal of Bone and Joint Surgery-American Volume.* 2010;92A(6):1398-1408.

20. Kim JG, Lee YS, Bae TS, et al. Tibiofemoral contact mechanics following posterior root of medial meniscus tear, repair, meniscectomy, and allograft transplantation. *Knee Surg Sports Traumatol Arthrosc.* 2012.

21. Muriuki MG, Tuason DA, Tucker BG, Harner CD. Changes in Tibiofemoral Contact Mechanics Following Radial Split and Vertical Tears of the Medial Meniscus An in Vitro Investigation of the Efficacy of Arthroscopic Repair. *Journal of Bone and Joint Surgery-American Volume.* 2011;93A(12):1089-1095.

22. Cox JS, Nye CE, Schaefer WW, Woodstein IJ. The degenerative effects of partial and total resection of the medial meniscus in dogs' knees. *Clin Orthop Relat Res.* 1975(109):178-183.

23. Barber FA, Herbert MA, Schroeder FA, Aziz-Jacobo J, Sutker MJ. Biomechanical testing of new meniscal repair techniques containing ultra high-molecular weight polyethylene suture. *Arthroscopy.* 2009;25(9):959-967.

24. Mariani PP. MENISCAL ROOT PATHOLOGY. ETIOLOGY, DIAGNOSIS AND TREATMENT. *Minerva Ortopedica E Traumatologica.* 2010;61(5):441-448.

25. Rockborn P, Messner K. Long-term results of meniscus repair and meniscectomy: a 13-year functional and radiographic follow-up study. *Knee Surgery Sports Traumatology Arthroscopy.* 2000;8(1):2-9.

26. McDermott I. Meniscal tears, repairs and replacement: their relevance to osteoarthritis of the. *Br J Sports Med.* 2011;45(4):292-297.

27. Lee YHD, Caborn DNM. A new technique for arthroscopic meniscus transplant using soft tissue fixation and anatomical meniscal root reinsertion. *Knee Surgery Sports Traumatology Arthroscopy.* 2012;20(5):904-908.

28. Noyes FR, Heckmann TP, Barber-Westin SD. Meniscus Repair and Transplantation: A Comprehensive Update. *Journal of Orthopaedic & Sports Physical Therapy.* 2012;42(3):274-290.

29. Klompmaker J, Jansen HW, Veth RP, Nielsen HK, de Groot JH, Pennings AJ. Porous implants for knee joint meniscus reconstruction: a preliminary study on. *Clin Mater.* 1993;14(1):1-11.

30. Klompmaker J, Veth RP, Jansen HW, et al. Meniscal repair by fibrocartilage in the dog: characterization of the repair. *Biomaterials.* 1996;17(17):1685-1691.

31. Klompmaker J, Veth RP, Jansen HW, Nielsen HK, de Groot JH, Pennings AJ. Meniscal replacement using a porous polymer prosthesis: a preliminary study in. *Biomaterials.* 1996;17(12):1169-1175.

32. Klompmaker J, Jansen HWB, Veth RPH, Degroot JH, Nijenhuis AJ, Pennings AJ. POROUS POLYMER IMPLANT FOR REPAIR OF MENISCAL LESIONS - A PRELIMINARY-STUDY IN DOGS. *Biomaterials.* 1991;12(9):810-816.

33. de Groot JH, de Vrijer R, Pennings AJ, Klompmaker J, Veth RP, Jansen HW. Use of porous polyurethanes for meniscal reconstruction and meniscal prostheses. *Biomaterials.* 1996;17(2):163-173.

34. de Groot JH, Zijlstra FM, Kuipers HW, et al. Meniscal tissue regeneration in porous 50/50. *Biomaterials.* 1997;18(8):613-622.

35. Welsing RT, van Tienen TG, Ramrattan N, et al. Effect on tissue differentiation and articular cartilage degradation of a polymer. *Am J Sports Med.* 2008;36(10):1978-1989.

36. Tienen TG, Heijkants RG, Buma P, De Groot JH, Pennings AJ, Veth RP. A porous polymer scaffold for meniscal lesion repair--a study in dogs. *Biomaterials.* 2003;24(14):2541-2548.

37. Tienen TG, Heijkants RG, de Groot JH, et al. Meniscal replacement in dogs. Tissue regeneration in two different materials with. *J Biomed Mater Res B Appl Biomater.* 2006;76(2):389-396.

38. Tienen TG, Heijkants RG, de Groot JH, et al. Replacement of the knee meniscus by a porous polymer implant: a study in dogs. *Am J Sports Med.* 2006;34(1):64-71.

39. Arnoczky SP. Building a meniscus - Biologic considerations. *Clinical Orthopaedics and Related Research.* 1999(367):S244-S253.

40. Bourke SL, Kohn J. Polymers derived from the amino acid L-tyrosine: polycarbonates, polyarylates and copolymers with poly(ethylene glycol). *Advanced Drug Delivery Reviews.* 2003;55(4):447-466.

41. Tovar N, Bourke S, Jaffe M, et al. A comparison of degradable synthetic polymer fibers for anterior cruciate ligament reconstruction. *Journal of Biomedical Materials Research Part A.* 2010;93A(2):738-747.

42. Tovar N, Murthy NS, Kohn J, Gatt C, Dunn M. ACL reconstruction using a novel hybrid scaffold composed of polyarylate fibers and collagen fibers. *Journal of Biomedical Materials Research Part A.* 2012;100A(11):2913-2920.

43. Sung HW, Chang WH, Ma CY, Lee MH. Crosslinking of biological tissues using genipin and/or carbodiimide. *Journal of Biomedical Materials Research Part A.* 2003;64A(3):427-438.

44. Zhang XW, Kotaki M, Okubayashi S, Sukigara S. Effect of electron beam irradiation on the structure and properties of electrospun PLLA and PLLA/PDLA blend nanofibers. *Acta Biomaterialia.* 2010;6(1):123-129.

45. Leonard DJ, Pick LT, Farrar DF, Dickson GR, Orr JF, Buchanan FJ. The modification of PLA and PLGA using electron-beam radiation. *Journal of Biomedical Materials Research Part A.* 2009;89A(3):567-574.

46. Li WJ, Danielson KG, Alexander PG, Tuan RS. Biological response of chondrocytes cultured in three-dimensional nanofibrous poly(epsilon-caprolactone) scaffolds. *Journal of Biomedical Materials Research Part A.* 2003;67A(4):1105-1114.

47. Riesle J, Hollander AP, Langer R, Freed LE, Vunjak-Novakovic G. Collagen in tissue-engineered cartilage: Types, structure, and crosslinks. *Journal of Cellular Biochemistry.* 1998;71(3):313-327.

48. Silver FH, Freeman JW, Seehra GP. Collagen self-assembly and the development of tendon mechanical properties. *Journal of Biomechanics.* 2003;36(10):1529-1553.

49. Zhang YZ, Lim CT, Ramakrishna S, Huang ZM. Recent development of polymer nanofibers for biomedical and biotechnological applications. *Journal of Materials Science-Materials in Medicine.* 2005;16(10):933-946.

50. Carnegie JA, Cabaca O. EXTRACELLULAR-MATRIX COMPOSITION AND RESILIENCE - 2 PARAMETERS THAT INFLUENCE THE INVITRO MIGRATION AND MORPHOLOGY OF RAT INNER CELL MASS-DERIVED CELLS. *Biology of Reproduction.* 1993;48(2):287-299.

51. Petersen W, Tillmann B. Collagenous fibril texture of the human knee joint menisci. *Anatomy and Embryology.* 1998;197(4):317-324.

52. Fithian DC, Kelly MA, Mow VC. MATERIAL PROPERTIES AND STRUCTURE-FUNCTION-RELATIONSHIPS IN THE MENISCI. *Clinical Orthopaedics and Related Research.* 1990(252):19-31.

53. Proctor CS, Schmidt MB, Whipple RR, Kelly MA, Mow VC. MATERIAL PROPERTIES OF THE NORMAL MEDIAL BOVINE MENISCUS. *Journal of Orthopaedic Research.* 1989;7(6):771-782.

54. Setton LA, Guilak F, Hsu EW, Vail TP. Biomechanical factors in tissue engineered meniscal repair. *Clinical Orthopaedics and Related Research.* 1999(367):S254-S272.

55. Li WJ, Mauck RL, Cooper JA, Yuan XN, Tuan RS. Engineering controllable anisotropy in electrospun biodegradable nanofibrous scaffolds for musculoskeletal tissue engineering. *Journal of Biomechanics.* 2007;40(8):1686-1693.

56. Beason DP, Connizzo BK, Dourte LM, et al. Fiber-aligned polymer scaffolds for rotator cuff repair in a rat model. *Journal of Shoulder and Elbow Surgery.* 2012;21(2):245-250.

57. Seedhom B, Hargreaves D. Transmission of the Load in the Knee Joint with Special Reference to the Role of the Menisci. *Engineering in Medicine.* 1979;8:220-228.

58. Spilker R, Donzelli P. A biphasic finite element model of the meniscus for stress-strain analysis. In: Mow V, Arnoczky S, Jackson D, eds. *Knee Meniscus: Basic and Clinical Foundations*. New York: Raven Press; 1992.

59. Spilker RL, Donzelli PS, Mow VC. A TRANSVERSELY ISOTROPIC BIPHASIC FINITE-ELEMENT MODEL OF THE MENISCUS. *Journal of Biomechanics.* 1992;25(9):1027-1045.

60. Jha BS, Ayres CE, Bowman JR, et al. Electrospun Collagen: A Tissue Engineering Scaffold with Unique Functional Properties in a Wide Variety of Applications. *Journal of Nanomaterials.* 2011.

61. Buerck J, Heissler S, Geckle U, et al. Resemblance of Electrospun Collagen Nanofibers to Their Native Structure. *Langmuir.* 2013;29(5):1562-1572.

62. Zeugolis DI, Khew ST, Yew ES, et al. Electro-spinning of pure collagen nano-fibres - just an expensive way to make gelatin? *Biomaterials.* 2008;29(15):2293-2305.

63. Electrospinning - Wikipedia, the free encyclopedia. 2013; http://en.wikipedia.org/wiki/Electrospinning.

64. Postlethwaite AE, Seyer JM, Kang AH. Chemotactic attraction of human fibroblasts to type I, II, and III collagens and collagen-derived peptides. *Proc Natl Acad Sci U S A.* 1978;75(2):871-875.

65. Heino J. The collagen family members as cell adhesion proteins. *Bioessays.* 2007;29(10):1001-1010.

66. Lima E. Open Source Electrospinning. http://engfac.cooper.edu/lima2/35, 2013.

67. Deitzel JM, Kleinmeyer J, Harris D, Tan NCB. The effect of processing variables on the morphology of electrospun nanofibers and textiles. *Polymer.* 2001;42(1):261-272.

68. Tuck SJ, Leach MK, Feng ZQ, Corey JM. Critical variables in the alignment of electrospun PLLA nanofibers. *Materials Science & Engineering C-Materials for Biological Applications.* 2012;32(7):1779-1784.

69. Dias JC, Ribeiro C, Sencadas V, Botelho G, Ribelles JLG, Lanceros-Mendez S. Influence of fiber diameter and crystallinity on the stability of electrospun poly(L-lactic acid) membranes to hydrolytic degradation. *Polymer Testing.* 2012;31(6):770-776.

70. Jacobs V, Anandjiwala RD, Maaza M. The Influence of Electrospinning Parameters on the Structural Morphology and Diameter of Electrospun Nanofibers. *Journal of Applied Polymer Science.* 2010;115(5):3130-3136.

71. Theron SA, Zussman E, Yarin AL. Experimental investigation of the governing parameters in the electrospinning of polymer solutions. *Polymer.* 2004;45(6):2017-2030.

72. Inai R, Kotaki M, Ramakrishna S. Structure and properties of electrospun PLLA single nanofibres. *Nanotechnology.* 2005;16(2):208-213.

73. Donahue TLH, Hull ML, Rashid MM, Jacobs CR. How the stiffness of meniscal attachments and meniscal material properties affect tibio-femoral contact pressure computed using a validated finite element model of the human knee joint. *Journal of Biomechanics.* 2003;36(1):19-34.

74. Yao J, Funkenbusch PD, Snibbe J, Maloney M, Lerner AL. Sensitivities of medial meniscal motion and deformation to material properties of articular cartilage, meniscus and meniscal attachments using design of experiments methods. *J Biomech Eng.* 2006;128(3):399-408.

75. Abraham AC, Donahue TLH. From meniscus to bone: A quantitative evaluation of structure and function of the human meniscal attachments. *Acta Biomaterialia.* 2013;9(5):6322-6329.

76. Hauch KN, Oyen ML, Odegard GM, Donahue TLH. Nanoindentation of the insertional zones of human meniscal attachments into underlying bone. *Journal of the Mechanical Behavior of Biomedical Materials.* 2009;2(4):339-347.

77. Moyer JT, Abraham AC, Donahue TLH. Nanoindentation of human meniscal surfaces. *Journal of Biomechanics.* 2012;45(13):2230-2235.

78. Moyer JT, Abraham AC, Killian ML, Donahue TLH, Asme. TRANSVERSE MECHANICAL PROPERTIES OF HUMAN LATERAL MENISCAL ATTACHMENTS. *Proceedings of the Asme Summer Bioengineering Conference, 2010.* 2010:693-694.

79. Villegas DF, Maes JA, Magee SD, Donahue TLH. Failure properties and strain distribution analysis of meniscal attachments. *Journal of Biomechanics.* 2007;40(12):2655-2662.

80. Villegas DF, Hansen TA, Liu DF, Donahue TLH. A quantitative study of the microstructure and biochemistry of the medial meniscal horn attachments. *Annals of Biomedical Engineering.* 2008;36(1):123-131.

81. Villegas DF, Donahue TLH. Collagen morphology in human meniscal attachments: A SEM study. *Connective Tissue Research.* 2010;51(5):327-336.

82. Maes JA, Donahue TLH. Time dependent properties of bovine meniscal attachments: Stress relaxation and creep. *Journal of Biomechanics.* 2006;39(16):3055-3061.

83. Chevrier A, Nelea M, Hurtig MB, Hoemann CD, Buschmann MD. Meniscus structure in human, sheep, and rabbit for animal models of meniscus repair. *J Orthop Res.* 2009;27(9):1197-1203.

84. Chiari C, Koller U, Dorotka R, et al. A tissue engineering approach to meniscus regeneration in a sheep model. *Osteoarthritis and Cartilage.* 2006;14(10):1056-1065.

85. Brophy RH, Cottrell J, Rodeo SA, Wright TM, Warren RF, Maher SA. Implantation of a synthetic meniscal scaffold improves joint contact mechanics in a partial meniscectomy cadaver model. *Journal of Biomedical Materials Research Part A.* 2010;92A(3):1154-1161.

86. Schepsis A. *Sports Medicine.* Philadelphia: Lippincott Williams & Wilkins; 2006.

87. Goodship AE, Birch HL. Cross sectional area measurement of tendon and ligament in vitro: a simple, rapid, non-destructive technique. *Journal of Biomechanics.* 2005;38(3):605-608.